

Ground states of the lattice-gas model on the triangular lattice with nearest- and next-nearest-neighbor pairwise interactions and with three-particle interaction: Ground states at boundaries of full-dimensional regions

Yu. I. Dublanych

Institute for Condensed Matter Physics, National Academy of Sciences of Ukraine, 1 Svientsitskii Street, 79011 Lviv, Ukraine

(Received 18 June 2011; revised manuscript received 8 September 2011; published 1 December 2011)

We analyze the ground states at boundaries of four-dimensional (full-dimensional) ground-state regions of the lattice-gas model on the infinite plane triangular lattice with nearest- and next-nearest-neighbor pairwise interactions and with additional interaction between three particles at the vertices of a nearest-neighbor triangle. In such a way we determine the ground states at fixed density of particles (coverage) and make the comparison to experiments possible. A surprisingly rich variety of structures is found: ordered periodic, ordered-but-aperiodic, disordered with various degree of disorder, and multiple-twin structures. The first-order and continuous phase transitions are identified. The degree of disorder for disordered ground states is analyzed. One of the most interesting results is the discovery of an infinite sequence of ground states at a boundary between two phases.

DOI: [10.1103/PhysRevE.84.061102](https://doi.org/10.1103/PhysRevE.84.061102)

PACS number(s): 05.50.+q, 75.10.Hk, 68.43.De, 68.43.Fg

I. INTRODUCTION

It is needless to say that lattice-gas models or equivalent spin models are widely used in different areas of physics. It is reasonable that the first step in the investigation of these models should be the determination of their ground states. These can be determined exactly if the model is not too complicated. There are numerous methods for determination of the ground states of lattice-gas models [1,2]. However, most of them have got two important shortcomings: (1) they permit to find only full-dimensional ground states, that is, the ground states in full-dimensional regions of the space of Hamiltonian parameters including the chemical potential (or the external field for the equivalent spin Hamiltonian); (2) they do not enable one to find disordered and ordered-but-aperiodic ground states (see, for instance, Ref. [2]). We developed a method that makes it possible to find all ground states at every point of the Hamiltonian parameter space.

Using this method, we solved the ground-state problem for the lattice-gas model on the triangular lattice with nearest- and next-nearest-neighbor pairwise interactions and with interaction between three particles at the vertices of the nearest-neighbor triangle. A complete solution was given in Ref. [3], though we constructed and analyzed only full-dimensional ground-state structures therein. Here we determine the ground states at the boundaries of full-dimensional regions. For the model that we consider, a full-dimensional region is a four-dimensional polyhedral cone. It has three types of boundaries: three (hyperfaces), two (faces), and one (edges) dimensional. We analyze the ground-state structures at all three-dimensional boundaries with the exception of two mutually symmetric ones where the sets of ground-state structures are so unconventional and complicated that they should be considered in a separate paper (anticipating things, we would like to report that we discovered continua of ground-state structures among which there are quasicrystalline ones). Only partial analysis of the ground states at these boundaries is provided in the present paper.

The investigation of the ground states in hyperfaces is important for two reasons: first, it enables us to identify the

first-order phase transitions driven by the chemical potential (or the external field for the spin model); second, it makes it possible to find the ground states at a fixed density of particles (coverage) and, hence, to link the theory with experiments.

Carrying out this analysis, we revealed a surprisingly rich variety of ground-state structures in hyperfaces; some of them are quite nontrivial. For instance, we found multiple-twin structures. We also found an infinite sequence of ground-state structures (very few examples of such sequences are known [4,5]) and proved that they cannot create an infinite sequence of full-dimensional ground states (so-called zero-temperature (top) devil's step [6]) at any additional interaction. Some interesting examples of ground-state structures at two-dimensional boundaries are also shown in the paper.

At the most boundaries, the ground-state structures turn out to be disordered. We analyzed the disorder at each boundary and showed that at many of them the entropy density is nonzero.

To increase the usability of our results, we constructed the ground-state phase diagrams where the first-order phase transitions are indicated.

The paper is organized as follows. In Sec. II, devoted to the summary of the results obtained in the previous paper, we present the solution of the ground-state problem in the form of a set of the so-called “basic rays” and the corresponding sets of configurations of the seven-site cluster in the form of flower; the full-dimensional ground-state structures are also presented in this section. In Sec. III, the basic rays and ground-state flower configurations are determined for the hyperfaces of the full-dimensional regions. Section IV is devoted to the analysis of the ground-state structures in the hyperfaces and transitions between full-dimensional phases. In Sec. V, some examples of the ground-state structures in two-dimensional faces of full-dimensional regions are presented. In Sec. VI, we analyze the degree of disorder and the existence of residual entropy for disordered ground states. In Sec. VII, we provide the ground-state phase diagrams and describe how to find ground-state structure at fixed interactions and density of particles. In Sec. VIII some conclusions are drawn.

TABLE I. Basic rays and basic sets of flower configurations for the spin model on the triangular lattice with nearest- and next-nearest-neighbor pairwise interactions and with three-spin nearest-neighbor interaction.

Basic ray $\mathbf{r}_i (h, J_1, J_2, J_\Delta)$	Basic set of flower configurations \mathbf{R}_i	Basic ray $\mathbf{r}_i^- (h, J_1, J_2, J_\Delta)$	Basic set of flower configurations \mathbf{R}_i^-
$\mathbf{r}_1 (0, 0, -1, 0)$		$\mathbf{r}_3^- (-6, 0, 1, 0)$	
$\mathbf{r}_2 (0, 0, 1, 0)$		$\mathbf{r}_4^- (0, 0, 1, -3)$	
$\mathbf{r}_3 (6, 0, 1, 0)$		$\mathbf{r}_5^- (-6, -2, 0, -3)$	
$\mathbf{r}_4 (0, 0, 1, 3)$		$\mathbf{r}_6^- (-2, -2, 2, -3)$	
$\mathbf{r}_5 (6, -2, 0, 3)$		$\mathbf{r}_7^- (-6, -4, 2, -3)$	
$\mathbf{r}_6 (2, -2, 2, 3)$		$\mathbf{r}_8^- (2, -1, 1, 0)$	
$\mathbf{r}_7 (6, -4, 2, 3)$		$\mathbf{r}_9^- (-4, 1, 1, 0)$	
$\mathbf{r}_8 (-2, -1, 1, 0)$		$\mathbf{r}_{10}^- (6, 2, 0, -1)$	
$\mathbf{r}_9 (4, 1, 1, 0)$		$\mathbf{r}_{11}^- (-6, 4, 2, -3)$	
$\mathbf{r}_{10} (-6, 2, 0, 1)$		$\mathbf{r}_{12}^- (2, 2, 2, -3)$	
$\mathbf{r}_{11} (6, 4, 2, 3)$		$\mathbf{r}_{13}^- (10, 14, 8, -15)$	
$\mathbf{r}_{12} (-2, 2, 2, 3)$			
$\mathbf{r}_{13} (-10, 14, 8, 15)$			

^a enter in structures with the neighborhoods shown in Fig. 1.

^b Symmetric condition.

II. SOLUTION OF THE GROUND-STATE PROBLEM AND FULL-DIMENSIONAL STRUCTURES

For the sake of convenience, we provide in this section the essential results of Ref. [3]. Thus, we consider the lattice-gas model with the Hamiltonian

$$H_{lg} = I_1 \sum_{NN} c_i c_j + I_2 \sum_{NNN} c_i c_j + I_\Delta \sum_{\Delta} c_i c_j c_k - \mu_{lg} \sum_i c_i, \quad (1)$$

where c_i are the lattice-gas occupation variables ($c_i = 1$ if the i th site is occupied by a particle and $c_i = 0$ otherwise); I_1 , I_2 are the nearest- and next-nearest-neighbor couplings, respectively; I_Δ is the three-particle interaction; and μ_{lg} denotes the chemical potential of particles. NN , NNN , and Δ denote the summation over the nearest neighbors, the next-nearest neighbors, and the nearest-neighbor triangles, respectively.

In view of the symmetry, it is more practical to consider the equivalent spin Hamiltonian

$$H_I = J_1 \sum_{NN} \sigma_i \sigma_j + J_2 \sum_{NNN} \sigma_i \sigma_j + J_\Delta \sum_{\Delta} \sigma_i \sigma_j \sigma_k - h \sum_i \sigma_i, \quad (2)$$

with the coupling constants and external field

$$J_1 = \frac{I_1 + I_\Delta}{4}, \quad J_2 = \frac{I_2}{4}, \quad J_\Delta = \frac{I_\Delta}{8}, \quad (3)$$

$$h = \frac{\mu_{lg}}{2} - 6(J_1 + J_2 - J_\Delta),$$

where $\sigma_i = 2c_i - 1 = \pm 1$ are spin variables. The spin Hamiltonian is invariant with respect to the inversion of all spins $\sigma = -1 \leftrightarrow \sigma = +1$ with simultaneous change of signs of J_Δ and h ; therefore, it suffices to consider only the $J_\Delta \geq 0$ case.

In the space of the Hamiltonian parameters, including the chemical potential (or the external field for the spin model), the region that corresponds to a ground-state structure of a lattice-gas (or spin) model is a convex polyhedral cone with the vertex at the origin of coordinates. Due to the convexity, the ground-state problem can be considered to be solved if all edges of full-dimensional polyhedral cones and all ground-state structures in these edges are determined. We called such edges “basic rays” and proved that model (2) has 24 basic rays. They are enumerated in Table I.

We also proved that every ground-state structure without defects in these rays, except two mutually symmetric rays \mathbf{r}_{13} and \mathbf{r}_{13}^- , can be constructed with a set of configurations of the seven-site cluster in the form of flower in such a manner that every flower in the structure should have one of the configurations belonging to the set, without any other restriction. Such a set is called “basic set” and we say that all ground-state structures in a ray are generated by the corresponding basic set of flower configurations. All basic sets of flower configurations are enumerated in Table I. In this table and thereafter, open circles represent vacancies, solid circles (except for light gray ones) represent particles, and light gray circles are undefined. For rays \mathbf{r}_{13} and \mathbf{r}_{13}^- the ground-state structures are constructed almost in the same way but an additional restriction should be taken into account: Flowers enter in structures with the neighborhoods shown in Fig. 1. Table I can be considered as a complete solution of the ground-state problem. It remains to construct global structures with local flower configurations. In many cases this is not very easy.

In Ref. [3] we found the full-dimensional regions (or more exactly, their basic rays) and the corresponding ground-state structures, which we called “full-dimensional structures.” We denoted them as in Ref. [2]. The structure with the bar over

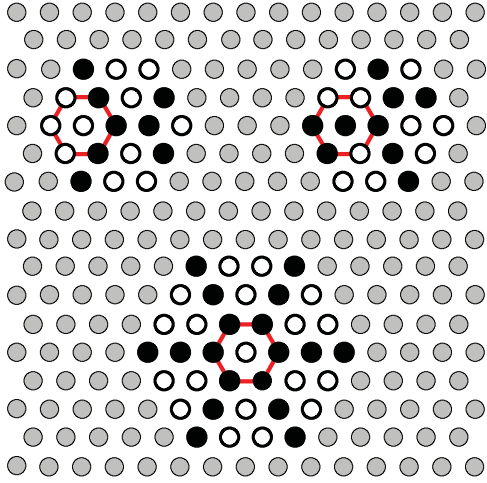
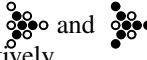


FIG. 1. (Color online) Neighborhoods for three flower configurations in ray \mathbf{r}_{13} .

its number is symmetric to the structure numbered without bar with respect to the particle-vacancy symmetry.

The structures with numbers without bars are depicted in Fig. 2, where the generating flower configurations are indicated, and, in the caption, the sets of basic rays are presented. Two of these structures (9 and 12) are disordered. For structures 11 and 12 an additional condition should be taken into account when constructing them with flowers: Configurations  are forbidden for structures 11 and 12, respectively.

In this paper we also use the notations of structures proposed by Kaburagi and Kanamori [7]: $S(p_0; p_1, p_2, p_3, \dots; p_\Delta)$, where p_0 is the number of particles per site, p_i ($i = 1, 2, 3, \dots$) provides the number of pairs of particles (per particle) that are i th neighbors, and p_Δ is the number of triplets of particles (per particle) that are nearest neighbors.

Now we can proceed to the construction of three-dimensional ground-state structures, that is, ground-state structures in the three-dimensional boundaries (3-faces or simply hyperfaces) of the full-dimensional regions.

III. BASIC RAYS AND GROUND-STATE FLOWER CONFIGURATIONS FOR HYPERFACES OF FULL-DIMENSIONAL REGIONS

Knowing the sets of basic rays for full-dimensional regions, one can easily find all hyperfaces. Two full-dimensional regions are neighboring (i.e., they have a common hyperface) if the intersection of their sets of basic vectors (rays) contains at least one triplet of linearly independent vectors. The basic vectors of this intersection generate the boundary; that is, the radius vector of every point of the boundary is a linear combination with non-negative coefficients (the so-called conical combination) of the vectors belonging to the intersection. The ground states at the boundary between these regions are generated by the flower configurations belonging to the intersection of all basic sets of flower configurations corresponding to the basic vectors which generate this boundary.

The sets of basic vectors (rays) generating hyperfaces of full-dimensional regions and the corresponding sets of

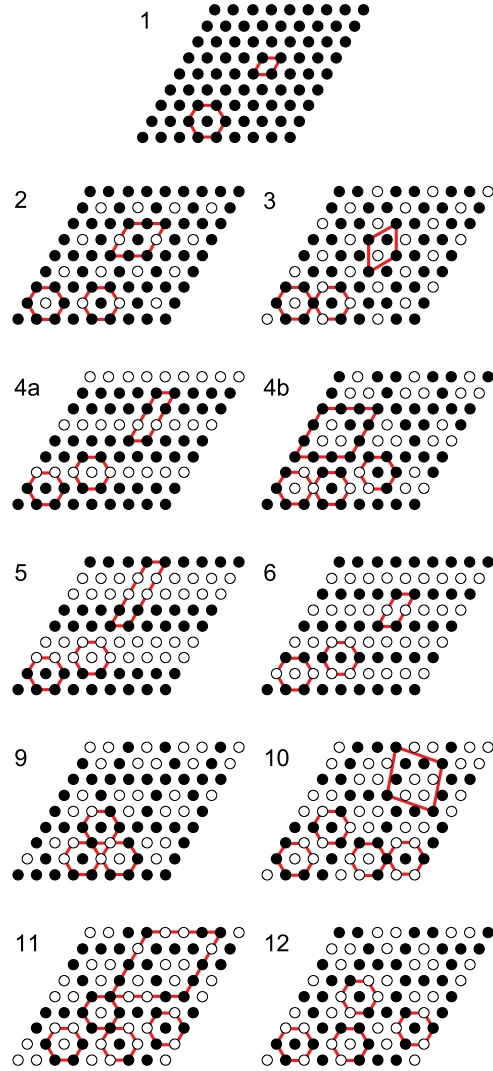


FIG. 2. (Color online) Full-dimensional structures (sets of basic rays are given): 1, $\{\mathbf{r}_1, \mathbf{r}_3, \mathbf{r}_5, \mathbf{r}_7, \mathbf{r}_4^-, \mathbf{r}_5^-, \mathbf{r}_6^-, \mathbf{r}_7^-, \mathbf{r}_8^-, \mathbf{r}_{10}^-\}$; 2, $\{\mathbf{r}_3, \mathbf{r}_4, \mathbf{r}_5, \mathbf{r}_6, \mathbf{r}_7, \mathbf{r}_9, \mathbf{r}_{11}, \mathbf{r}_{10}^-\}$; 3, $\{\mathbf{r}_1, \mathbf{r}_4, \mathbf{r}_5, \mathbf{r}_{10}, \mathbf{r}_{11}, \mathbf{r}_{10}^-\}$; 4a, $\{\mathbf{r}_2, \mathbf{r}_3, \mathbf{r}_9, \mathbf{r}_4^-, \mathbf{r}_6^-, \mathbf{r}_8^-, \mathbf{r}_{10}^-, \mathbf{r}_{12}^-\}$; 4b, $\{\mathbf{r}_2, \mathbf{r}_3, \mathbf{r}_6, \mathbf{r}_7, \mathbf{r}_9, \mathbf{r}_8^-\}$; 5, $\{\mathbf{r}_2, \mathbf{r}_6, \mathbf{r}_7, \mathbf{r}_8, \mathbf{r}_6^-, \mathbf{r}_7^-, \mathbf{r}_8^-\}$; 6, $\{\mathbf{r}_2, \mathbf{r}_9, \mathbf{r}_{10}, \mathbf{r}_{11}, \mathbf{r}_{12}, \mathbf{r}_{13}, \mathbf{r}_9^-, \mathbf{r}_{10}^-, \mathbf{r}_{11}^-, \mathbf{r}_{12}^-, \mathbf{r}_{13}^-\}$; 9, $\{\mathbf{r}_2, \mathbf{r}_4, \mathbf{r}_6, \mathbf{r}_9, \mathbf{r}_{11}, \mathbf{r}_{12}\}$; 10, $\{\mathbf{r}_4, \mathbf{r}_{10}, \mathbf{r}_{12}, \mathbf{r}_{13}\}$; 11, $\{\mathbf{r}_4, \mathbf{r}_{10}, \mathbf{r}_{11}, \mathbf{r}_{13}\}$; and 12, $\{\mathbf{r}_4, \mathbf{r}_{11}, \mathbf{r}_{12}, \mathbf{r}_{13}\}$. Unit cells (for ordered structures) and generating flower configurations are indicated. Structures 9 and 12 are disordered.

flower configurations generating the ground states in these hyperfaces are presented in Table II. The minimal energy configurations incompatible with other configurations of the set and with themselves (i.e., with their copies) are separated by the symbol |. In the first column of Table II the full-dimensional regions for which the hyperface is the common boundary are indicated. In the last column the conditions for existence of the boundary in the plane (h, J_2) are presented. The content of the fourth column of Table II is explained hereinafter.

Let us notice that only some of the hyperfaces are shown in Table II. All other hyperfaces can be obtained from the given ones by substituting every region and every flower configuration for the symmetric region and flower configuration. Basic ray \mathbf{r}_i ($3 \leq i \leq 13$) should be replaced by basic ray \mathbf{r}_i^- and vice versa. The total number of hyperfaces is equal to 60.

TABLE II. Basic rays and flower configurations for hyperfaces of the full-dimensional ground-state regions of the spin model on the triangular lattice with nearest- and next-nearest-neighbor pairwise interactions and with three-spin nearest-neighbor interaction. For continuous transitions dimensionality of disorder is indicated in parentheses.

Regions	Basic rays of the hyperface	Flower configurations for ground states in the hyperface	Transition between phases	Conditions for existence in the plane (h, J_2)
1, $\bar{1}$	$\mathbf{r}_1, \mathbf{r}_5, \mathbf{r}_7, \mathbf{r}_7^-, \mathbf{r}_5^-$		Jump	$\frac{3}{2}J_1 < J_\Delta < -\frac{3}{2}J_1$
1, 2	$\mathbf{r}_5, \mathbf{r}_7, \mathbf{r}_3, \mathbf{r}_{10}^-$		Cont. (2)	$-J_\Delta < \frac{3}{4}J_1, -J_\Delta < \frac{1}{2}J_1$
$\bar{1}$, 2	$\mathbf{r}_4, \mathbf{r}_6, \mathbf{r}_7, \mathbf{r}_5$		Jump	$0 < -\frac{3}{4}J_1 < J_\Delta$
1, 3	$\mathbf{r}_1, \mathbf{r}_5, \mathbf{r}_{10}^-$		Jump	$-J_\Delta < \frac{3}{2}J_1, -J_\Delta < \frac{1}{2}J_1$
$\bar{1}$, 3	$\mathbf{r}_4, \mathbf{r}_5, \mathbf{r}_1, \mathbf{r}_{10}$		Jump	$-J_\Delta < -\frac{1}{2}J_1, -J_\Delta < \frac{3}{2}J_1$
$\bar{1}$, $4a$	$\mathbf{r}_4, \mathbf{r}_6, \mathbf{r}_8, \mathbf{r}_3^-, \mathbf{r}_{10}$		Cont. (1)	$J_1 < 0, -J_\Delta < 0$
1, $4b$	$\mathbf{r}_3, \mathbf{r}_7, \mathbf{r}_8^-$		Cont. (2)	$0 < J_\Delta < -\frac{3}{4}J_1$
$\bar{1}$, 5	$\mathbf{r}_7, \mathbf{r}_6, \mathbf{r}_8, \mathbf{r}_7^-$		Cont. (1)	$0 < J_\Delta < -\frac{3}{2}J_1$
2, 3	$\mathbf{r}_5, \mathbf{r}_4, \mathbf{r}_{11}, \mathbf{r}_{10}^-$		Jump	$-J_\Delta < \frac{1}{2}J_1, -J_\Delta < \frac{3}{2}J_1$
$\bar{2}$, $4a$	$\mathbf{r}_{10}, \mathbf{r}_3^-, \mathbf{r}_9^-$		Two jumps	$0 < J_\Delta < \frac{1}{2}J_1$
2, $4b$	$\mathbf{r}_3, \mathbf{r}_7, \mathbf{r}_6, \mathbf{r}_9$		Jump	$-J_\Delta < 0, -J_\Delta < \frac{3}{4}J_1$
2, 6	$\mathbf{r}_9, \mathbf{r}_{11}, \mathbf{r}_{10}^-$		Cont. (2)	$\frac{1}{2}J_1 < J_\Delta < \frac{3}{4}J_1$
2, 9	$\mathbf{r}_4, \mathbf{r}_6, \mathbf{r}_9, \mathbf{r}_{11}$		Jump + cont. (2)	$-J_\Delta < 0, -J_\Delta < \frac{3}{2}J_1$
3, $\bar{3}$	$\mathbf{r}_1, \mathbf{r}_{10}, \mathbf{r}_{10}^-$		Jump	$-\frac{1}{2}J_1 < J_\Delta < \frac{1}{2}J_1$
3, 6	$\mathbf{r}_{10}, \mathbf{r}_{11}, \mathbf{r}_{10}^-$		Cont. (1)	$-\frac{1}{2}J_1 < J_\Delta < \frac{3}{4}J_1$
3, 11	$\mathbf{r}_4, \mathbf{r}_{10}, \mathbf{r}_{11}$		Jump	$0 < \frac{1}{2}J_1 < J_\Delta$
$4a$, $4b$	$\mathbf{r}_3, \mathbf{r}_9, \mathbf{r}_2, \mathbf{r}_8^-$		Jump	$J_\Delta = 0$
$4a$, 5	$\mathbf{r}_2, \mathbf{r}_6, \mathbf{r}_8$		Cont. (1)	$0 < J_\Delta < -\frac{3}{2}J_1$
$4a$, 6	$\mathbf{r}_2, \mathbf{r}_{12}, \mathbf{r}_{10}, \mathbf{r}_9^-$		Cont. (1)	$0 < J_\Delta < -\frac{3}{2}J_1$
$4a$, 9	$\mathbf{r}_4, \mathbf{r}_6, \mathbf{r}_2, \mathbf{r}_{12}$		Cont. (2)	$-J_\Delta < \frac{3}{2}J_1, -J_\Delta < -\frac{3}{2}J_1$
$4a$, 10	$\mathbf{r}_4, \mathbf{r}_{10}, \mathbf{r}_{12}$		Cont. (1) + twins	$0 < \frac{1}{2}J_1 < J_\Delta$
$4b$, 5	$\mathbf{r}_2, \mathbf{r}_6, \mathbf{r}_7, \mathbf{r}_8^-$		Jump + twins	$0 < J_\Delta < -\frac{3}{2}J_1$
$4b$, 9	$\mathbf{r}_2, \mathbf{r}_6, \mathbf{r}_9$		Cont. (2)	$-J_\Delta < 0, -J_\Delta < \frac{3}{2}J_1$
6, 9	$\mathbf{r}_2, \mathbf{r}_9, \mathbf{r}_{11}, \mathbf{r}_{12}$		Cont. (1)	$0 < J_\Delta < \frac{3}{2}J_1$
6, 10	$\mathbf{r}_{10}, \mathbf{r}_{12}, \mathbf{r}_{13}$		Jump	$\frac{1}{2}J_1 < J_\Delta < \frac{3}{2}J_1$
6, 11	$\mathbf{r}_{10}, \mathbf{r}_{11}, \mathbf{r}_{13}$		Jump	$\frac{1}{2}J_1 < J_\Delta < \frac{15}{14}J_1$
6, 12	$\mathbf{r}_{11}, \mathbf{r}_{12}, \mathbf{r}_{13}$		Jump	$\frac{3}{4}J_1 < J_\Delta < \frac{3}{2}J_1$
9, 12	$\mathbf{r}_4, \mathbf{r}_{11}, \mathbf{r}_{12}$		Special case	$0 < \frac{3}{4}J_1 < J_\Delta$
10, 11	$\mathbf{r}_4, \mathbf{r}_{10}, \mathbf{r}_{13}$		Cont. (1)	$0 < \frac{3}{4}J_1 < J_\Delta$
10, 12	$\mathbf{r}_4, \mathbf{r}_{12}, \mathbf{r}_{13}$		Jump	$0 < \frac{15}{14}J_1 < J_\Delta$
11, 12	$\mathbf{r}_4, \mathbf{r}_{11}, \mathbf{r}_{13}$		Cascade of jumps	$0 < \frac{3}{4}J_1 < J_\Delta$

^a enter in structures with the neighborhoods shown in Fig. 1.

Basic rays for every hyperface are enumerated in such an order that every pair of neighboring rays (the first one and the last one are also neighboring) generates a two-dimensional face of the three-dimensional hyperface. The maximal number of faces is five: for the hyperface between regions 1 and $4a$ ($\bar{1}$ and $4a$) as well as between regions 1 and $\bar{1}$. In what follows, instead of “hyperface between regions A and B” we write “hyperface (A, B).”

IV. GROUND-STATE STRUCTURES IN THE HYPERFACES AND TRANSITIONS BETWEEN FULL-DIMENSIONAL PHASES

A. Jump and continuous transition between two neighboring phases

Our method makes it possible to analyze phase transitions at zero temperature. This is based on the following statement:

If with the flower configurations of a set corresponding to the boundary between two neighboring full-dimensional regions it is possible to construct only two structures (one of which is a ground-state structure on one side of the boundary and another on the other side), then between these full-dimensional phases there is a first-order phase transition driven by the chemical potential (or the external field for the spin model) or the phase separation in the case of fixed density of particles. The following is an example. With flowers and which are the ground-state flower configurations at the boundary between regions 3 and 11, one can construct only two structures without defects: structures 3 and 11. Any other ground state at this boundary represents a phase separation between structures 3 and 11 and contains an infinitesimal quantity of flowers with nonminimal energy. Hence, there is a first-order phase transition between phases 3 and 11. In Table II such transitions are indicated by the word “Jump.”

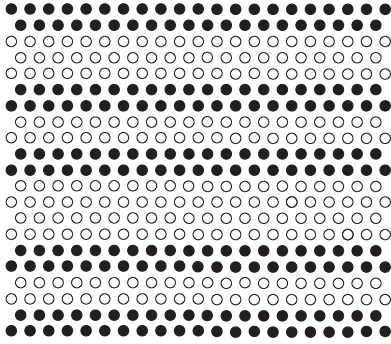


FIG. 3. A mixture of phases $\bar{1}$ and 5.

If with the flower configurations of a set corresponding to the boundary between two neighboring full-dimensional regions one can construct an infinite number of structures with the density of particles (or the magnetization per site) which can take each value between densities of particles for two neighboring phases, then the phase transition from one of these phases to another is continuous. The transition between phases $\bar{1}$ and 5 is a typical example of such a transition. The ground states between these regions are generated by three flower configurations: $\begin{smallmatrix} \bullet & \bullet & \bullet \\ \bullet & \bullet & \bullet \\ \bullet & \bullet & \bullet \end{smallmatrix}$, $\begin{smallmatrix} \bullet & \bullet & \bullet \\ \bullet & \bullet & \bullet \\ \bullet & \bullet & \bullet \end{smallmatrix}$, and $\begin{smallmatrix} \bullet & \bullet & \bullet \\ \bullet & \bullet & \bullet \\ \bullet & \bullet & \bullet \end{smallmatrix}$. These ground states represent a mixture of structures $\bar{1}$ and 5 in arbitrary ratios (Fig. 3). Such simple mixtures of two structures take place for many hyperfaces, for instance, between regions $\bar{1}$ and $4a$, $\bar{4a}$ and 6, 6 and 9, etc. In these hyperfaces the disorder is one dimensional. This means that there is an order in one direction, for instance, in horizontal direction (see Fig. 3), and a disorder in the other one. Hence, in these hyperfaces there is no residual entropy (per site).

However, intermediate structures between two phases are not always a simple mixture of the leftmost and rightmost limiting structures. In Fig. 4(a) an intermediate structure between phases 3 and 6 is shown. The ground-state structures at this boundary are generated by the following set of flower configurations: $\begin{smallmatrix} \bullet & \bullet & \bullet \\ \bullet & \bullet & \bullet \\ \bullet & \bullet & \bullet \end{smallmatrix}$, $\begin{smallmatrix} \bullet & \bullet & \bullet \\ \bullet & \bullet & \bullet \\ \bullet & \bullet & \bullet \end{smallmatrix}$, and $\begin{smallmatrix} \bullet & \bullet & \bullet \\ \bullet & \bullet & \bullet \\ \bullet & \bullet & \bullet \end{smallmatrix}$. These structures represent a hybrid of structures 3 and 6, rather than their simple mixture. Notice that the subset containing only three flower configurations, $\begin{smallmatrix} \bullet & \bullet & \bullet \\ \bullet & \bullet & \bullet \\ \bullet & \bullet & \bullet \end{smallmatrix}$, $\begin{smallmatrix} \bullet & \bullet & \bullet \\ \bullet & \bullet & \bullet \\ \bullet & \bullet & \bullet \end{smallmatrix}$, and $\begin{smallmatrix} \bullet & \bullet & \bullet \\ \bullet & \bullet & \bullet \\ \bullet & \bullet & \bullet \end{smallmatrix}$, generates the ordered structure shown in Fig. 4(b). Another example of a hybrid structure is shown in Fig. 5. It is a hybrid of structures 10 and 11, which is a ground-state structure at the boundary between the corresponding regions. In Table II continuous phase transitions are indicated by the abbreviation ‘‘Cont.’’

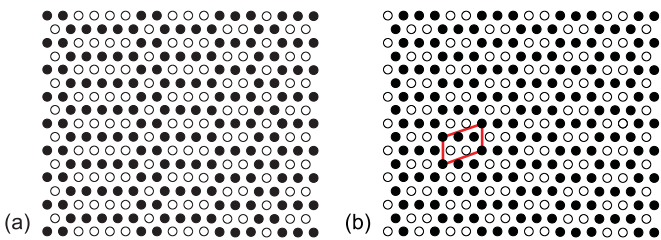


FIG. 4. (Color online) (a) A hybrid of phases 3 and 6. (b) Ordered structure at the boundary between regions 3 and 6, generated by the set of flower configurations $\begin{smallmatrix} \bullet & \bullet & \bullet \\ \bullet & \bullet & \bullet \\ \bullet & \bullet & \bullet \end{smallmatrix}$, $\begin{smallmatrix} \bullet & \bullet & \bullet \\ \bullet & \bullet & \bullet \\ \bullet & \bullet & \bullet \end{smallmatrix}$, and $\begin{smallmatrix} \bullet & \bullet & \bullet \\ \bullet & \bullet & \bullet \\ \bullet & \bullet & \bullet \end{smallmatrix}$.

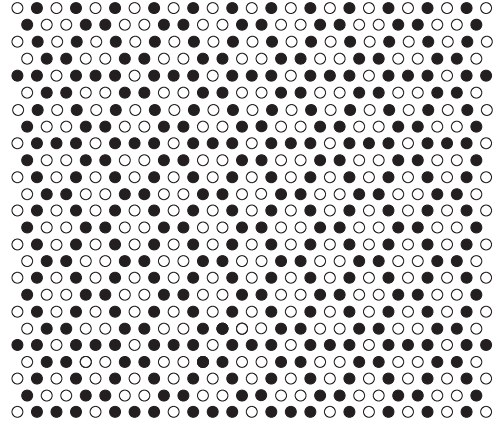


FIG. 5. A hybrid disordered structure at the boundary between regions 10 and 11.

The cases described above do not exhaust all of the diversity of possible types of ground-state structures in hyperfaces of full-dimensional regions. In what follows we consider some of these types.

B. Two jumps between regions $\bar{2}$ and $\bar{4a}$

Not quite a typical situation occurs at the boundary between phases $\bar{2}$ and $4a$. The following flower configurations have the minimal energy at this boundary: $\begin{smallmatrix} \bullet & \bullet & \bullet \\ \bullet & \bullet & \bullet \\ \bullet & \bullet & \bullet \end{smallmatrix}$, $\begin{smallmatrix} \bullet & \bullet & \bullet \\ \bullet & \bullet & \bullet \\ \bullet & \bullet & \bullet \end{smallmatrix}$, $\begin{smallmatrix} \bullet & \bullet & \bullet \\ \bullet & \bullet & \bullet \\ \bullet & \bullet & \bullet \end{smallmatrix}$, and $\begin{smallmatrix} \bullet & \bullet & \bullet \\ \bullet & \bullet & \bullet \\ \bullet & \bullet & \bullet \end{smallmatrix}$. In addition to structures $\bar{2}$ and $4a$ these configurations generate the structure $S(\frac{7}{25}; \frac{3}{7}, 0; 0)$ (Fig. 6). Hence, there are two first-order phase transitions between phases $\bar{2}$ and $4a$. The intermediate structure is all that remains from the infinite sequence of structures at the boundary between these two phases in $J_{\Delta} = 0$ case (see. Ref. [4]).

C. Jump and continuous transition between regions 2 and 9

An interesting set of structures occurs in the hyperface (2, 9). These structures contain only four flower configurations: $\begin{smallmatrix} \bullet & \bullet & \bullet \\ \bullet & \bullet & \bullet \\ \bullet & \bullet & \bullet \end{smallmatrix}$, $\begin{smallmatrix} \bullet & \bullet & \bullet \\ \bullet & \bullet & \bullet \\ \bullet & \bullet & \bullet \end{smallmatrix}$, and $\begin{smallmatrix} \bullet & \bullet & \bullet \\ \bullet & \bullet & \bullet \\ \bullet & \bullet & \bullet \end{smallmatrix}$. However, in addition to structures 2 and 9, one can construct with these configurations an infinite number of structures and among them the structure $S(\frac{12}{19}; \frac{7}{4}, \frac{3}{2}, \frac{1}{2})$ (Fig. 7), which is the closest to the structure $S(\frac{3}{4}; 2, 2; \frac{2}{3})$ (structure 2). The rest of structures are mixtures of the first structure with structure 9 [Figs. 8(a) and 8(b)]. Therefore, there are two phase transitions between phases 2 and 9: (1) the jump from phase 2 into the intermediate phase $S(\frac{12}{19}; \frac{7}{4}, \frac{3}{2}, \frac{1}{2})$ and (2) the continuous transition from this phase to phase 9.

The ground-state disorder in the hyperface (2, 9) is two-dimensional since in some ground-state structures in

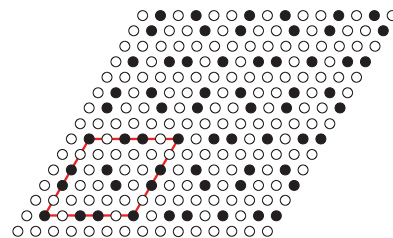


FIG. 6. (Color online) Structure $S(\frac{7}{25}; \frac{3}{7}, 0; 0)$ in the hyperface $(\bar{2}, \bar{4a})$.

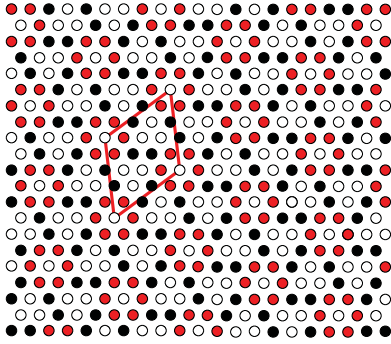


FIG. 7. (Color online) Structure $S(\frac{12}{19}; \frac{7}{4}, \frac{3}{2}, \frac{1}{2})$ in the hyperface (2, 9).

this hyperface one can make local changes which do not lead to the appearance of other flower configurations. It is seen from Fig. 8(b) where “waterwheels” in the middle of regular hexagons can be orientated clockwise as well as counterclockwise. Hence, there is a macroscopic degeneracy and therefore a residual entropy per site in the hyperface (2, 9).

D. Ordered multiple-twin structures

Let us consider the ground-state structures in the hyperface $(4a, 10)$. They are generated by the following flower configurations: flower_1 , flower_2 , flower_3 , flower_4 , and flower_5 . With these flowers one can construct not only the infinite number of structures which are a hybrid of structures $4a$ and 10 [Fig. 9(a)] but also other two structures depicted in Figs. 9(b) and 9(c). These ordered structures do not have global translational symmetry, though they are not quasicrystals. These are ordered multiple-twin structures. As one can see, they do not need a defect (a flower configuration with nonminimal energy) for their formation.

An ordered structure without global translational symmetry also occurs in the hyperface (5, 4b). It is generated by the set of flower configurations flower_1 , flower_2 , flower_3 , flower_4 , and flower_5 , if one starts with configuration flower_1 . This structure is composed of

two domains of structure $4b$ in such a manner that the domain wall has zero energy of formation (Fig. 10). An infinite number of multiple-twin structures occur in the hyperface (9, 12). We will analyze them in another paper.

E. Infinite sequence of structures in the hyperface (11, 12)

An extraordinary set of ground-state structures occurs in the hyperface (11, 12). They are constructed with flowers flower_1 , flower_2 , flower_3 , flower_4 , and flower_5 in such a way that two larger configurations flower_6 and flower_7 do not appear. This additional condition for the set of flowers is equivalent to the condition that flowers flower_1 and flower_2 should have the neighborhoods depicted in Fig. 1.

If flower flower_1 is removed from this set, then the remaining flowers generate structures 12. Hence, let us start with configuration flower_2 . It is easy to see that we obtain an infinite sequence T_n ($n = 0, 1, 2, \dots$) of structures. Member zero of this sequence is structure 11. The two following structures are depicted in Figs. 11(a) and 11(b). The unit cell of structure T_n has dimension $\sqrt{16 + 27n^2} \times \sqrt{16 + 27n^2}$. Structures T_n are degenerated: They all, except for the zero one and the limiting one, occur only at the boundary between regions 11 and 12, where they have the same energy. Can this degeneracy be removed by some pairwise interactions? We have calculated for structures T_n the number of i -th-neighbor pairs per particle up to $i = 10$:

$$\begin{aligned} p_0 &= \frac{15n^2 + 9}{27n^2 + 16}, & p_\Delta &= \frac{2n^2}{15n^2 + 9}, & p_1 &= \frac{21n^2 + 12}{15n^2 + 9}, \\ p_2 &= \frac{24n^2 + 18}{15n^2 + 9}, & p_3 &= \frac{21n^2 + 12}{15n^2 + 9}, & p_4 &= \frac{66n^2 + 36}{15n^2 + 9}, \\ p_5 &= \frac{18n^2 + 12}{15n^2 + 9}, & p_6 &= \frac{24n^2 + 12}{15n^2 + 9}, \end{aligned} \quad (4)$$

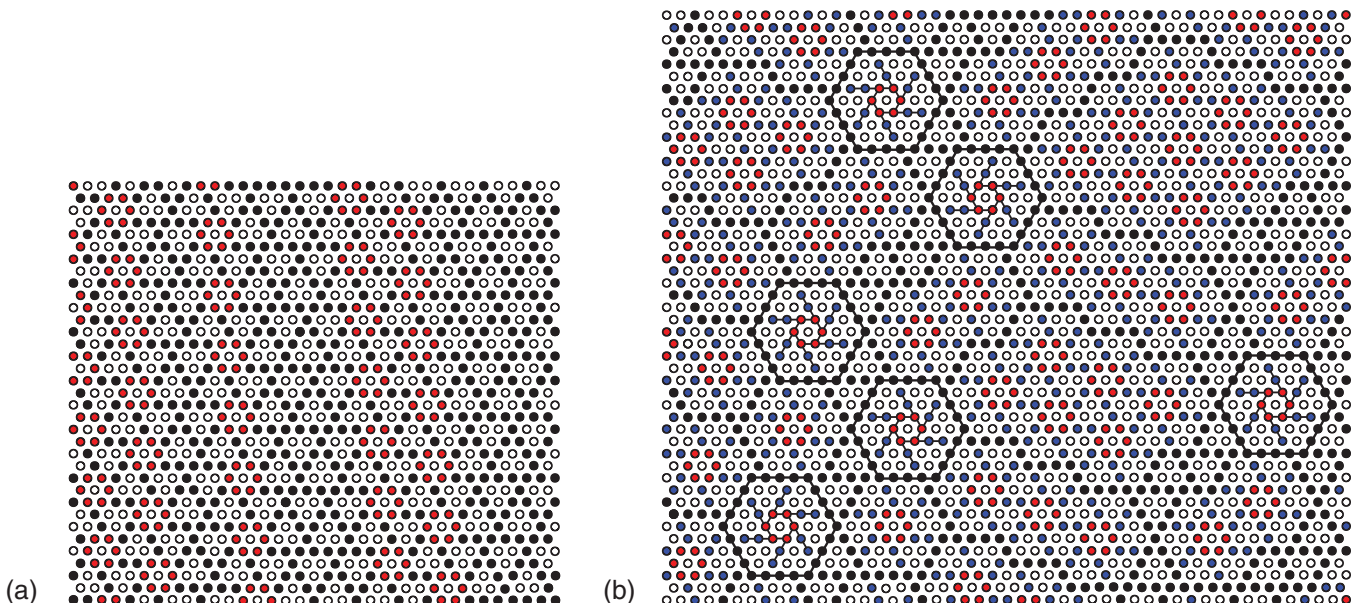


FIG. 8. (Color online) Mixtures of structures in the hyperface (2, 9). (a) Strip mixture of structures $S(\frac{12}{19}; \frac{7}{4}, \frac{3}{2}, \frac{1}{2})$ and 9; (b) zigzag mixture of these structures. The “waterwheel” in each hexagon can be orientated clockwise as well as counterclockwise.

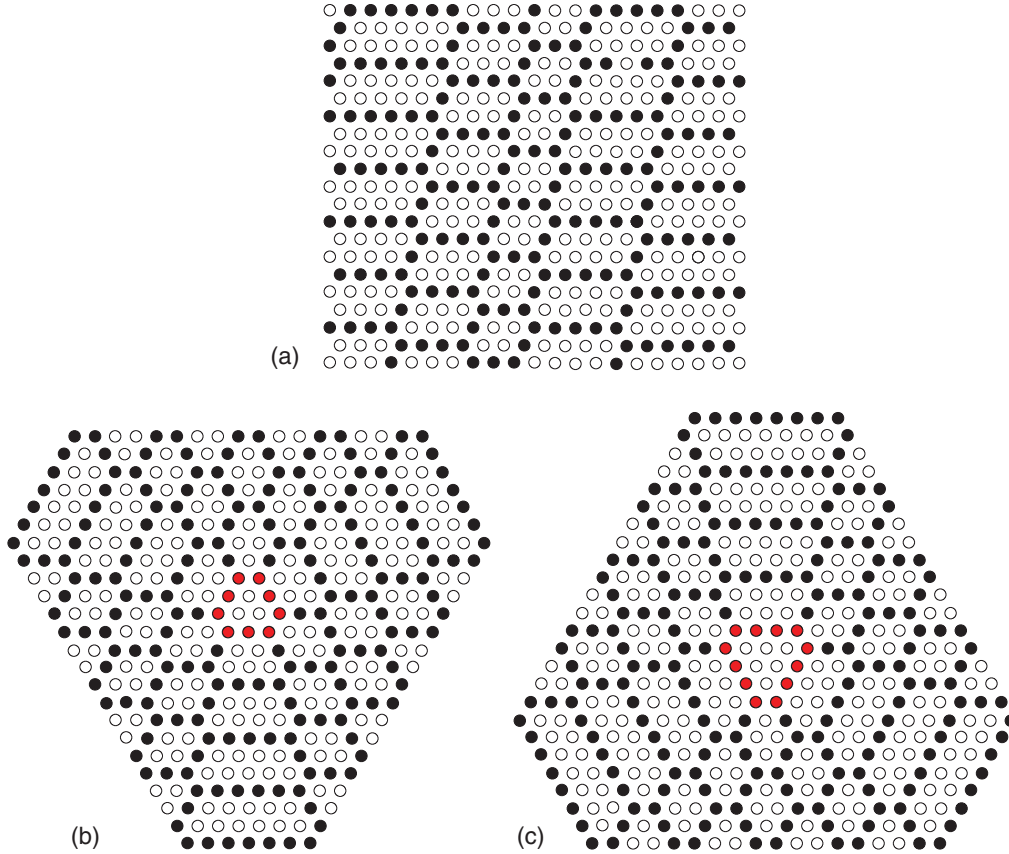


FIG. 9. (Color online) Ground-state structures in the hyperface $(\overline{4a}, 10)$. (a) A hybrid disordered structure; (b),(c) two six-domain structures.

$$p_7 = \frac{42n^2 + 24}{15n^2 + 9}, \quad p_8 = \frac{33n^2 - 3n + 27}{15n^2 + 9},$$

$$p_9 = \frac{42n^2 + 3n + 36}{15n^2 + 9}, \quad p_{10} = \frac{48n^2 + 6n + 24}{15n^2 + 9}.$$

Pairwise interactions up to seventh neighbors remove neither the degeneracy at the boundary between phases 11 and 12 nor the degeneracy of structures 12. The reason is that a term proportional to n does not enter the expressions for the number of i th-neighbor pairs per particle. Really, if, for some sequence of structures, $p_i(n)$ and $p_\Delta(n)$ have the form

$$p_0(n) = \frac{a_0n^2 + b_0}{cn^2 + d}, \quad p_i(n) = \frac{a_in^2 + b_i}{a_0n^2 + b_0},$$

$$p_\Delta(n) = \frac{a_\Delta n^2 + b_\Delta}{a_0n^2 + b_0} \quad (n = 0 - \infty),$$
(5)

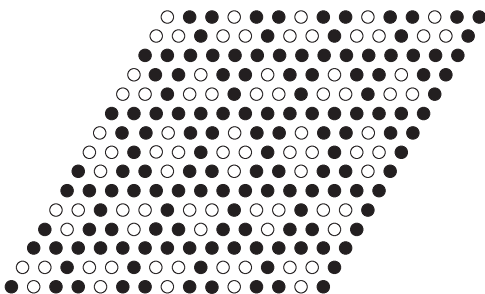


FIG. 10. Two-domain structure in the hyperface $(5, 4b)$.

then, in the line $E_0 = E_\infty$, where E_0 and E_∞ are energies per site for zero and limiting structures, respectively, all structures of the sequence have the same energy. This is easy to show using the expression for the energy per site of a structure $S(p_0; p_1, p_2, p_3, \dots; p_\Delta)$:

$$E = \sum_i p_0 p_i I_i + p_0 p_\Delta I_\Delta - p_0 \mu_{lg}, \quad i = 1, 2, \dots \quad (6)$$

The expression for p_8 contains a term proportional to n . Therefore, the interaction between eighth neighbors removes the degeneracy. However, it is not difficult to show that even this interaction does not generate a zero-temperature devil's step, that is, a sequence of full-dimensional ground-states. A question arises: Does an interaction (pairwise or many particle) exist which, lifting the degeneracy at the boundary between regions 11 and 12, can lead to the appearance of a zero-temperature devil's step? Let us prove that such an interaction does not exist.

F. Conditions for existence of a zero-temperature devil's step

Let us consider an infinite sequence of structures on a two-dimensional lattice. These structures are characterized by the number of particles per site $p_0(n)$ and the numbers of some clusters of particles per particle $p_i(n)$ (a cluster can represent, for instance, a pair of particles, a triplet

of nearest-neighbor particles, etc.). Since the lattice is two-dimensional, these values have the form

$$p_0(n) = \frac{a_0 n^2 + b_0 n + c_0}{r n^2 + s n + t}, \quad p_i(n) = \frac{a_i n^2 + b_i n + c_i}{a_0 n^2 + b_0 n + c_0}. \quad (7)$$

The equation of the boundary between phases m and $m + 1$ is

$$E(m) = E(m + 1) \quad (8)$$

or

$$\mu_{lg} = \frac{\sum_i [p_0(m + 1)p_i(m + 1) - p_0(m)p_i(m)]I_i}{p_0(m + 1) - p_0(m)}. \quad (9)$$

Here I_i are interaction parameters. The interactions can be pairwise as well as many-particle. Substituting expressions (7) for $p_0(m)$ and $p_i(m)$ into Eq. (9), we get

$$\mu_{lg} = \frac{\sum_i \{(-a_i s + b_i r)m^2 + [-a_i(s + 2t) + (b_i + 2c_i)r]m - (a_i + b_i)t + c_i(r + s)\}I_i}{\{(-a_0 s + b_0 r)m^2 + [-a_0(s + 2t) + (b_0 + 2c_0)r]m - (a_0 + b_0)t + c_0(r + s)\}}. \quad (10)$$

Let us analyze this expression. If the condition

$$-a_0 s + b_0 r \neq 0 \quad (11)$$

is satisfied, then the limit $\lim_{m \rightarrow \infty} \mu_{lg}$ is finite; therefore, the devil's step (an infinite sequence of ground states) can exist and the equation of its boundary is

$$\mu_{lg} = \frac{\sum_i (-a_i s + b_i r)I_i}{-a_0 s + b_0 r}. \quad (12)$$

If

$$-a_0 s + b_0 r = 0, \quad \sum_i (-a_i s + b_i r)I_i \neq 0, \quad (13)$$

then, at $m \rightarrow \infty$, the expression for μ_{lg} diverges and, hence, an infinite sequence of phases cannot exist. If the conditions

$$-a_0 s + b_0 r = 0, \quad \sum_i (-a_i s + b_i r)I_i = 0, \quad -a_0 t + c_0 r \neq 0 \quad (14)$$

are satisfied, then the infinite sequence of structures occurs only in the hyperface between the zero phase and the

limiting phase of the sequence. The equation of this boundary reads

$$\mu_{lg} = \frac{\sum_i (c_i r - a_i t)I_i}{c_0 r - a_0 t}. \quad (15)$$

All structures of the sequence, including the zero one and the limiting one, have the same energy at this boundary.

These general considerations lead to the conclusion that structures T_n cannot create the zero-temperature devil's step at any additional interactions, since the $-a_0 s + b_0 r \neq 0$ condition is not satisfied for this sequence of structures. However, in our model, these structures have equal energy at the boundary between phases 11 and 12 (zero and limiting structures of sequence T_n). One can check that condition (11) is fulfilled for all devil's steps known at present (see Refs. [5,6]).

G. Ground-state structures in the hyperface (9,12) (partial analysis)

Ground-state structures in the hyperface (9,12) are generated by flower configurations \odot , \ominus , \oplus , \otimes , and \circledast . The

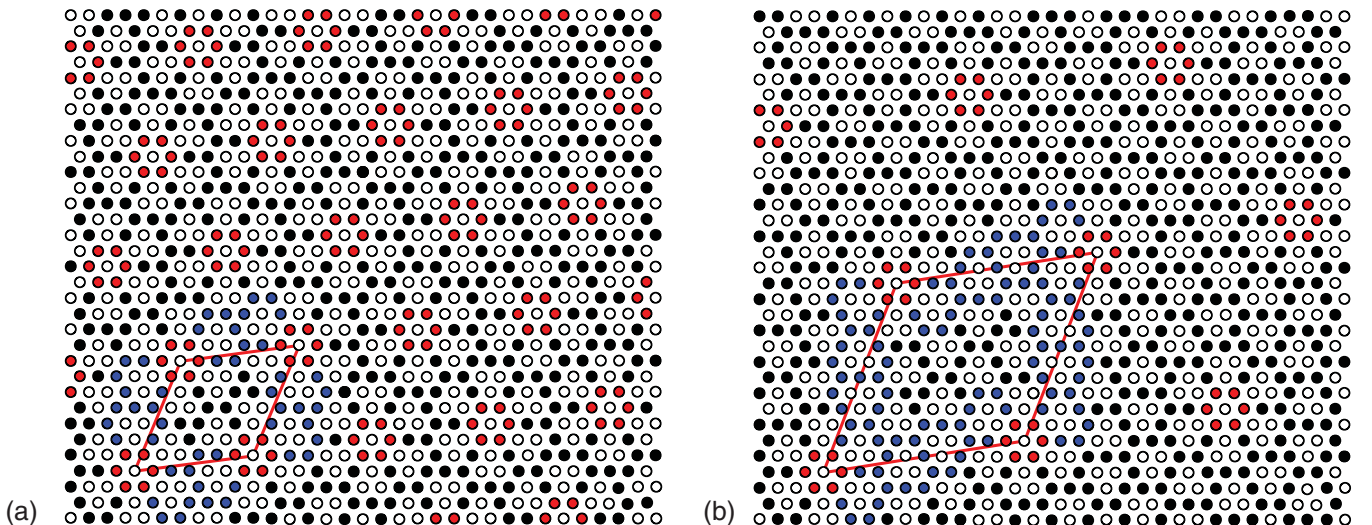


FIG. 11. (Color online) Structures (a) T_1 and (b) T_2 in the hyperface (11, 12). Colored sites facilitate understanding the principle of construction for structures T_n .

set of these structures is so sophisticated, unconventional, and interesting that we will discuss it in a separate paper. Here we present only partial analysis of these ground states.

All ground-state structures in the hyperface (9,12) can be divided into three groups: (1) structures which contain configuration $\odot\odot\odot$ but do not contain configuration $\bullet\bullet\bullet$, (2) structures which contain configuration $\bullet\bullet\bullet$ but do not contain configuration $\odot\odot\odot$, and (3) structures which contain both configurations $\odot\odot\odot$ and $\bullet\bullet\bullet$. Our aim is to show that the third-neighbor pairwise interaction (small enough) lifts partially the degeneracy in hyperfaces (9,12) separating all three groups of structures. For this purpose we use the relations derived in Ref. [8] and in such a way we demonstrate that they are really useful.

Let the fractional contents of configurations $\odot\odot\odot$, $\bullet\bullet\bullet$, $\odot\bullet\odot$, $\odot\odot\bullet$, and $\bullet\odot\odot$ in a structure that they generate be k_1, k_2, k_3, k_4 , and k_5 , respectively. Along with the notation $S(p_0; p_1, p_2, p_3, p_\Delta)$ of a structure we use the notation $[k_1, k_2, k_3, k_4, k_5]$ (as in Ref. [3]). The values k_i are not independent; they are connected by the following linear relations [8]:

$$\begin{aligned} 2k_1 - k_2 + k_4 &= 0, \\ 2k_1 - 3k_2 + 3k_3 + 2k_4 + 2k_5 &= 0, \\ k_1 + k_2 + k_3 + k_4 + k_5 &= 1, \end{aligned} \quad (16)$$

which can be rewritten in the form

$$\begin{aligned} 13k_1 &= 3 - 7k_4 - k_5, \\ 13k_2 &= 6 - k_4 - 2k_5, \\ 13k_3 &= 4 - 5k_4 - 10k_5. \end{aligned} \quad (17)$$

Hence, the characteristics of a structure (within the framework of the cluster considered) can be expressed in terms of only two of the five values k_i , for instance, k_4 and k_5 :

$$\begin{aligned} p_0 &= \frac{1}{7}(3k_1 + 4k_2 + 4k_3 + 4k_4 + 5k_5) = \frac{7 + k_4 + 2k_5}{13}, \\ p_1 &= \frac{1}{4p_0}(2k_1 + 3k_2 + 3k_3 + 4k_4 + 6k_5) \\ &= \frac{9 + 5k_4 + 10k_5}{13p_0} = 5 - \frac{2}{p_0}, \\ p_2 &= \frac{1}{2p_0}(2k_2 + 3k_3 + k_4 + 2k_5) \\ &= \frac{12 - 2k_4 - 4k_5}{13p_0} = -2 + \frac{2}{p_0}, \\ p_\Delta &= \frac{1}{3p_0}(k_4 + 2k_5) = \frac{13}{3} - \frac{7}{3p_0}. \end{aligned} \quad (18)$$

As one can see, the values p_1 , p_2 , and p_Δ depend on particle density p_0 only; therefore, the energy of every structure from the set of structures under consideration is a function of p_0 (interactions and chemical potential being fixed). However, the number of third neighbors per particle p_3 depends not only on p_0 :

$$\begin{aligned} p_3 &= \frac{1}{p_0}(k_1 + k_2 + k_4 + 2k_5) = \frac{9 + 5k_4 + 23k_5}{13p_0} \\ &= \frac{23}{2} - \frac{11 + k_4}{2p_0} = 5 + \frac{k_5 - 2}{p_0}. \end{aligned} \quad (19)$$

Just for this reason the third-neighbor pairwise interaction (small enough) partially lifts the degeneracy in hyperfaces (9,12).

Let us express k_i ($i = 1 - 4$) in terms of p_0 and k_5 :

$$\begin{aligned} k_1 &= 4 - 7p_0 + k_5, & k_2 &= 1 - p_0, \\ k_3 &= 3 - 5p_0, & k_4 &= -7 + 13p_0 - 2k_5. \end{aligned} \quad (20)$$

The first of these equalities yields that at $p_0 > \frac{4}{7}$ the value k_5 should be greater than zero; hence, the corresponding structures contain configuration $\odot\odot\odot$.

If the third-neighbor interaction (small enough) is repulsive ($I_3 > 0$), then k_5 should be as small as possible. For $\frac{5}{9} \leq p_0 < \frac{4}{7}$ the minimal value of k_5 is zero; $p_3 = 12 - \frac{2}{p_0}$ and the energy density is

$$\begin{aligned} E &= p_0(5I_1 - 2I_2 + 5I_3 + \frac{13}{3}I_\Delta - \mu_{lg}) \\ &\quad - 2I_1 + 2I_2 - 2I_3 - \frac{7}{3}I_\Delta. \end{aligned} \quad (21)$$

Hence, in the hyperface

$$5I_1 - 2I_2 + 5I_3 + \frac{13}{3}I_\Delta - \mu_{lg} = 0 \quad (22)$$

the ground-state structures are generated by configuration $\odot\odot\odot$, $\odot\bullet\odot$, $\odot\odot\bullet$, and $\bullet\odot\odot$. For $\frac{4}{7} < p_0 \leq \frac{3}{5}$ the minimal value of k_5 is $k_5 = 7p_0 - 4$ ($k_1 = 0$); $p_3 = 12 - \frac{6}{p_0}$ and the energy density is

$$\begin{aligned} E &= p_0(5I_1 - 2I_2 + 12I_3 + \frac{13}{3}I_\Delta - \mu_{lg}) \\ &\quad - 2I_1 + 2I_2 - 6I_3 - \frac{7}{3}I_\Delta; \end{aligned} \quad (23)$$

therefore, in the hyperface

$$5I_1 - 2I_2 + 12I_3 + \frac{13}{3}I_\Delta - \mu_{lg} = 0 \quad (24)$$

the ground-state structures are generated by configurations $\odot\odot\odot$, $\odot\bullet\odot$, $\odot\odot\bullet$, and $\bullet\odot\odot$.

If $p_0 = \frac{4}{7}$, then it follows from Eqs. (16)

$$k_1 = k_5, \quad k_2 = \frac{3}{7}, \quad k_3 = \frac{1}{7}, \quad k_4 = \frac{3}{7} - 2k_5. \quad (25)$$

If $I_3 > 0$, then $k_5 = k_1 = 0$ and the ground-state structure is generated by configurations $\odot\odot\odot$, $\odot\bullet\odot$, and $\odot\odot\bullet$. This structure

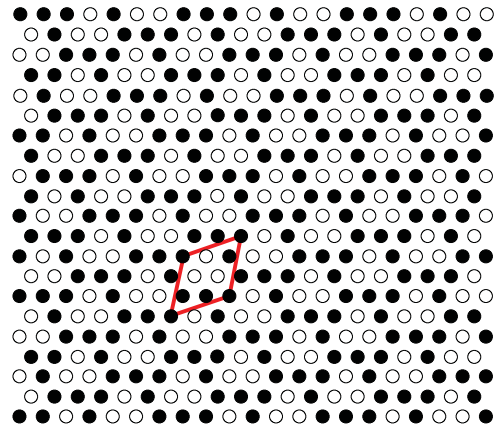


FIG. 12. (Color online) Structure $S(\frac{4}{7}; \frac{3}{2}, \frac{3}{2}, \frac{3}{2}, \frac{1}{4})([0, \frac{3}{7}, \frac{1}{7}, \frac{3}{7}, 0])$ in the hyperface (9, 12). This structure becomes full dimensional if the third-neighbor interaction is included into the Hamiltonian.

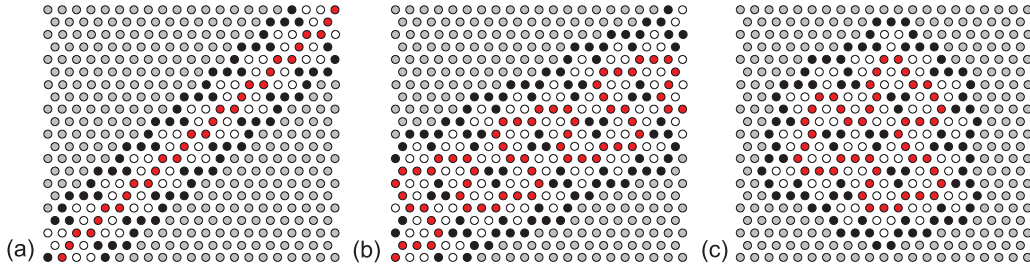


FIG. 13. (Color online) Examples of (a),(b) infinite and (c) closed chains created by occupied sites of configurations $\textcircled{\bullet\bullet}$ (in red) in structures at the boundary of phases 9 and 12.

is depicted in Fig. 12. It is full dimensional if $I_3 \neq 0$ and is realized between hyperfaces (22) and (24).

Hence, the repulsive third-neighbor interaction separates the first two groups of ground-state structures in the hyperface (9,12) without eliminating any of these structures. The structure with $p_0 = \frac{4}{7}$ becomes full dimensional in the five-dimensional space $(I_1, I_2, I_3, I_\Delta, \mu_{lg})$.

We showed that the first and second groups represent continua of structures among which there are quasicrystalline ones but the analysis of these continua is so difficult and interesting that we will provide it in a separate paper. We hope that it will shed new light on two long-standing problems: infinitely adaptive structures and the formation of quasicrystals.

As to the third group of structures in the hyperface (9,12), they are difficult to construct and we investigated them only partially. Let us note that in structures generated by configurations $\textcircled{\bullet\bullet}$, $\textcircled{\bullet\bullet\bullet}$, $\textcircled{\bullet\bullet\bullet\bullet}$, and $\textcircled{\bullet\bullet\bullet\bullet\bullet}$, the occupied sites of configurations $\textcircled{\bullet\bullet}$ create chains which are either infinite [Figs. 13(a) and 13(b)] or closed [Fig. 13(c)]. We suppose (we did not manage to prove it) that, in the third group, only structures containing the simplest infinite and closed chains created by occupied sites of configurations $\textcircled{\bullet\bullet}$ are possible (see Figs. 14 and 15). If this is true, then only the structure depicted in Fig. 14 “survives” at the boundary between phases 9 and 12 if additional interaction $I_3 < 0$ is included into the Hamiltonian.

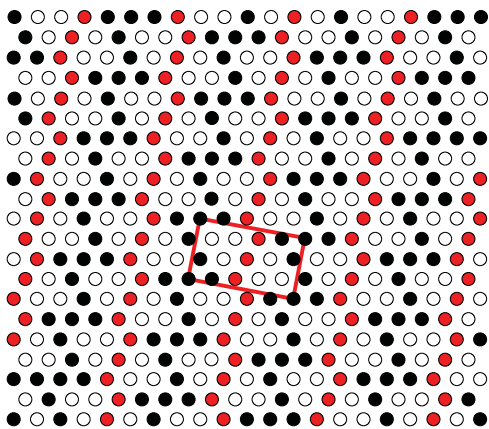


FIG. 14. (Color online) Structure $S(\frac{4}{7}; \frac{3}{2}, \frac{3}{2}, \frac{13}{8}; \frac{1}{4})$ ($[\frac{1}{14}, \frac{3}{7}, \frac{1}{7}, \frac{2}{7}, \frac{1}{14}]$) in the hyperface (9, 12).

V. SOME EXAMPLES OF STRUCTURES IN 2-FACES OF FULL-DIMENSIONAL REGIONS

We have investigated ground states of model (1) in full-dimensional regions and in the hyperfaces of these regions, except for the hyperface (9, 12), where the ground-state structures were investigated only partially. To provide the full description of the ground states of the model, one also needs to describe ground states in the faces and edges (2-faces and 1-faces) of the full-dimensional regions although they are not so important for practical use as ground states at the hyperfaces. The faces of the full-dimensional regions and the corresponding sets of flower configurations which generate all ground-state structures in these faces are presented in Table III. Faces are denoted by pairs of basic vectors which generate them. For each face the full-dimensional regions bounded by this face are indicated. It should be noticed that only 33 faces from total 64 ones are enumerated in Table III. The remaining faces are symmetrical to the given ones.

It is much more difficult to describe the ground-state structures in the faces than in the hyperfaces because the degeneracy in the faces is greater. Therefore, we provide only some examples but not the full description.

In each face, there exist from three to five full-dimensional phases as well as structures which are mixtures or hybrids of two or more full-dimensional structures. However, some new structures can also appear. A striking example of a face where new immiscible structures appear is the face bounded by rays \mathbf{r}_3 and \mathbf{r}_9 , where $J_\Delta = 0$. (We denote it by $\{\mathbf{r}_3, \mathbf{r}_9\}$). In this face an infinite sequence of structures exists. We studied this sequence in Ref. [4].

There are also faces where two full-dimensional structures intermix but do not mix with a third full-dimensional structure. Face $\{\mathbf{r}_{10}, \mathbf{r}_{12}\}$ is an example of such a situation. In this face, structure 6 mixes with structure $\overline{4a}$ but does not mix with structure 10. Structures 10 and $\overline{4a}$ create a set of hybrid structures depicted in Fig. 9(a). In this face, there are also two ordered multiple-twin structures described above. They do not mix with any other structure. Hence, in face $\{\mathbf{r}_{10}, \mathbf{r}_{12}\}$ there are only those ground-state structures which are also in the hyperfaces bounded by this face.

Face $\{\mathbf{r}_{10}, \mathbf{r}_{11}\}$ is an example of a face where all three full-dimensional structures, 3, 6, and 11, create a hybrid structure. In this face structure 11 mixes neither with structure 3 nor with structure 6. It mixes only with the structure depicted in Fig. 4(b), which is a hybrid of structures 3 and 6. This is easy to prove, showing that in face $\{\mathbf{r}_{10}, \mathbf{r}_{11}\}$, in addition

TABLE III. Ground states in two-dimensional faces of full-dimensional regions for the spin model on the triangular lattice with nearest- and next-nearest-neighbor pairwise interactions and with three-spin nearest-neighbor interaction.

Face	Ground-state flowers for the face	Disorder	Full-dimensional structures	Coordinates in the plane (h, J_2)	Conditions for existence in the plane (h, J_2)
$\{\mathbf{r}_1, \mathbf{r}_5\}$		0	$1, \bar{1}, 3$	$J_\Delta = -\frac{3}{2}J_1, h = -3J_1$	$J_1 < 0, J_2 < 0$
$\{\mathbf{r}_1, \mathbf{r}_{10}^-\}$		0	$1, 3, \bar{3}$	$J_\Delta = -\frac{1}{2}J_1, h = \frac{1}{3}J_1$	$-J_1 < 0, J_2 < 0$
$\{\mathbf{r}_2, \mathbf{r}_6\}$		2	$\bar{4}a, 4b, 5, 9$	$J_\Delta = -\frac{3}{2}J_1, h = -J_1$	$-J_2 < J_1 < 0$
$\{\mathbf{r}_2, \mathbf{r}_8^-\}$		1	$4a, 4b, 5$	$J_\Delta = 0, h = -2J_1$	$-J_2 < J_1 < 0$
$\{\mathbf{r}_2, \mathbf{r}_9\}$		2	$4a, 4b, 6, 9$	$J_\Delta = 0, h = 4J_1$	$0 < J_1 < J_2$
$\{\mathbf{r}_2, \mathbf{r}_{12}\}$		2	$6, 9, \bar{4}a$	$J_\Delta = \frac{3}{2}J_1, h = -J_1$	$0 < J_1 < J_2$
$\{\mathbf{r}_3, \mathbf{r}_7\}$		2	$1, 2, 4b$	$J_\Delta = -\frac{3}{4}J_1,$ $2h - 3J_1 - 12J_2 = 0$	$J_1 < 0, J_1 < -2J_2$
$\{\mathbf{r}_3, \mathbf{r}_8^-\}$		2	$1, 4a, 4b$	$J_\Delta = 0, h - 4J_1 - 6J_2 = 0$	$-J_2 < J_1 < 0$
$\{\mathbf{r}_3, \mathbf{r}_9\}$		0	$2, 4a, 4b$	$J_\Delta = 0, h + 2J_1 - 6J_2 = 0$	$0 < J_1 < J_2$
$\{\mathbf{r}_3, \mathbf{r}_{10}^-\}$		2	$1, 2, 4a$	$J_\Delta = -\frac{1}{2}J_1,$ $h - 3J_1 - 6J_2 = 0$	$-J_1 < 0, -J_2 < 0$
$\{\mathbf{r}_4, \mathbf{r}_5\}$		0	$\bar{1}, 2, 3$	$(-3J_1, \frac{1}{2}J_1 + \frac{1}{3}J_\Delta)$	$0 < -\frac{3}{2}J_1 < J_\Delta$
$\{\mathbf{r}_4, \mathbf{r}_6\}$		2	$\bar{1}, 2, \bar{4}a, 9$	$(-J_1, -\frac{1}{2}J_1 + \frac{1}{3}J_\Delta)$	$0 < -\frac{3}{2}J_1 < J_\Delta$
$\{\mathbf{r}_4, \mathbf{r}_{10}\}$		2	$\bar{1}, 3, \bar{4}a, 10, 11$	$(-3J_1, -\frac{1}{6}J_1 + \frac{1}{3}J_\Delta)$	$0 < \frac{1}{2}J_1 < J_\Delta$
$\{\mathbf{r}_4, \mathbf{r}_{11}\}$		2	$2, 3, 9, 11, 12$	$(\frac{3}{2}J_1, \frac{1}{4}J_1 + \frac{1}{3}J_\Delta)$	$0 < \frac{3}{4}J_1 < J_\Delta$
$\{\mathbf{r}_4, \mathbf{r}_{12}\}$		2	$\bar{4}a, 9, 10, 12$	$(-J_1, \frac{1}{2}J_1 + \frac{1}{3}J_\Delta)$	$0 < \frac{3}{2}J_1 < J_\Delta$
$\{\mathbf{r}_4, \mathbf{r}_{13}\}$		2	$10, 11, 12$	$(-\frac{5}{7}J_1, \frac{3}{14}J_1 + \frac{1}{3}J_\Delta)$	$0 < \frac{15}{14}J_1 < J_\Delta$
$\{\mathbf{r}_5, \mathbf{r}_7\}$		2	$1, \bar{1}, 2$	$(2J_\Delta, -J_1 - \frac{2}{3}J_\Delta)$	$-\frac{3}{4}J_1 < J_\Delta < -\frac{3}{2}J_1$
$\{\mathbf{r}_5, \mathbf{r}_{10}^-\}$		2	$1, 2, 3$	$(6J_1 + 6J_\Delta, 0)$	$-J_\Delta < \frac{1}{2}J_1,$ $-J_\Delta < \frac{3}{2}J_1$
$\{\mathbf{r}_6, \mathbf{r}_7\}$		1	$\bar{1}, 2, 4b, 5$	$(-2J_1 - \frac{2}{3}J_\Delta, \frac{2}{3}J_\Delta)$	$-\frac{3}{4}J_1 < J_\Delta < -\frac{3}{2}J_1$
$\{\mathbf{r}_6, \mathbf{r}_8\}$		1	$\bar{1}, \bar{4}a, 5$	$(2J_1 + 2J_\Delta, -J_1)$	$0 < J_\Delta < -\frac{3}{2}J_1$
$\{\mathbf{r}_6, \mathbf{r}_9\}$		2	$2, 4b, 9$	$(4J_1 + \frac{10}{3}J_\Delta, J_1 + \frac{4}{3}J_\Delta)$	$-J_\Delta < \frac{3}{2}J_1, -J_\Delta < 0$
$\{\mathbf{r}_7, \mathbf{r}_7^-\}$		1	$1, \bar{1}, 5$	$(2J_\Delta, -\frac{1}{2}J_1)$	$\frac{3}{4}J_1 < J_\Delta < -\frac{3}{4}J_1$
$\{\mathbf{r}_7, \mathbf{r}_8^-\}$		2	$1, 4b, 5$	$(-2J_1 - \frac{2}{3}J_\Delta, -J_1 - \frac{2}{3}J_\Delta)$	$0 < J_\Delta < -\frac{3}{4}J_1$
$\{\mathbf{r}_9^-, \mathbf{r}_{10}\}$		2	$\bar{2}, \bar{4}a, 6$	$(-4J_1 + 2J_\Delta, J_1 - 2J_\Delta)$	$0 < J_\Delta < \frac{1}{2}J_1$
$\{\mathbf{r}_9, \mathbf{r}_{11}\}$		2	$2, 6, 9$	$(4J_1 - \frac{10}{3}J_\Delta, J_1 - \frac{2}{3}J_\Delta)$	$0 < J_\Delta < \frac{3}{4}J_1$
$\{\mathbf{r}_{10}, \mathbf{r}_{10}^-\}$		2	$3, \bar{3}, 6$	$(-6J_\Delta, 0)$	$-\frac{1}{2}J_1 < J_\Delta < \frac{1}{2}J_1$
$\{\mathbf{r}_{10}, \mathbf{r}_{11}\}$		1	$3, 6, 11$	$(-12J_1 + 18J_\Delta, -J_1 + 2J_\Delta)$	$\frac{1}{2}J_1 < J_\Delta < \frac{3}{4}J_1$
$\{\mathbf{r}_{10}^-, \mathbf{r}_{11}\}$		2	$2, 3, 6$	$(\frac{12}{5}J_1 - \frac{6}{5}J_\Delta, \frac{1}{5}J_1 + \frac{2}{5}J_\Delta)$	$-\frac{1}{2}J_1 < J_\Delta < \frac{3}{4}J_1$
$\{\mathbf{r}_{10}, \mathbf{r}_{12}\}$		1	$6, \bar{4}a, 10$	$(-4J_1 + 2J_\Delta, -\frac{1}{2}J_1 + J_\Delta)$	$\frac{1}{2}J_1 < J_\Delta < \frac{3}{2}J_1$
$\{\mathbf{r}_{10}, \mathbf{r}_{13}\}$		1	$6, 10, 11$	$(-5J_1 + 4J_\Delta, -\frac{1}{2}J_1 + J_\Delta)$	$\frac{1}{2}J_1 < J_\Delta < \frac{15}{14}J_1$
$\{\mathbf{r}_{11}, \mathbf{r}_{12}\}$		1	$6, 9, 12$	$(4J_1 - \frac{10}{3}J_\Delta, \frac{2}{3}J_\Delta)$	$\frac{3}{4}J_1 < J_\Delta < \frac{3}{2}J_1$
$\{\mathbf{r}_{11}, \mathbf{r}_{13}\}$		0	$6, 11, 12$	$(\frac{20}{3}J_1 - \frac{62}{9}J_\Delta, \frac{1}{3}J_1 + \frac{2}{9}J_\Delta)$	$\frac{3}{4}J_1 < J_\Delta < \frac{15}{14}J_1$
$\{\mathbf{r}_{12}, \mathbf{r}_{13}\}$		0	$6, 10, 12$	$(-\frac{2}{3}J_\Delta, -\frac{1}{2}J_1 + J_\Delta)$	$\frac{15}{14}J_1 < J_\Delta < \frac{3}{2}J_1$

^a and enter in structures with the neighborhoods shown in Fig. 1.

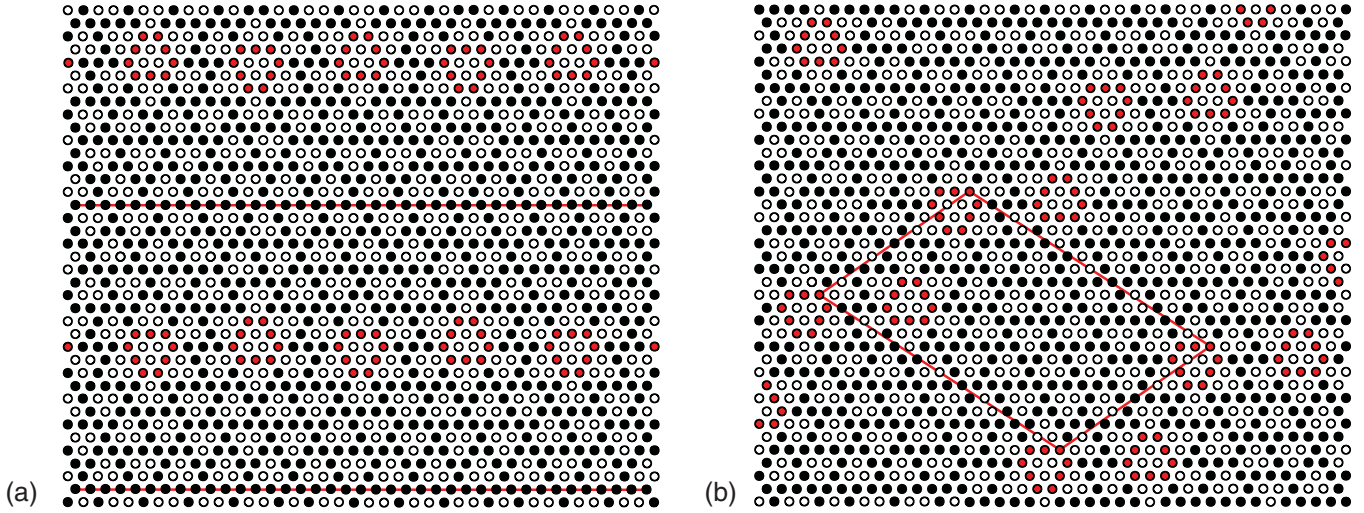


FIG. 15. (Color online) Structure (a) $S(\frac{13}{22}, \frac{21}{13}, \frac{18}{13}, \frac{5}{13})([\frac{3}{154}, \frac{9}{22}, \frac{1}{22}, \frac{57}{22}, \frac{12}{77}])$ and (b) $S(\frac{73}{124}, \frac{117}{73}, \frac{102}{73}, \frac{27}{73})([\frac{3}{124}, \frac{51}{124}, \frac{7}{124}, \frac{45}{124}, \frac{9}{62}])$ in the hyperface (9, 12). Structure (a) is partially disordered, since the strips (bounded by horizontal lines) can be shifted relative to each other in the horizontal direction.

to structures 3 and 6 and also their mixtures [Fig. 4(a)], only the structures constructed with the blocks depicted in Fig. 12(a) are possible. There is one-dimensional disorder in this face. A hybrid of structures 3, 6, and 11 is shown in Fig. 16(b).

The ground states in face $\{\mathbf{r}_4, \mathbf{r}_{10}\}$ are interesting as well. They are generated with the following set of flower configurations: . These flowers create a tiling of the lattice by hexagons of arbitrary dimensions (Fig. 17). The empty phase can be considered as the infinite hexagon. It is easy to see that the disorder in this face is two dimensional since some finite areas can be altered without altering their neighborhoods and within the framework of the given set of flower configurations. Hence, in this face, the entropy per site is nonzero.

Let us make some more examples. In face $\{\mathbf{r}_2, \mathbf{r}_8\}$ the ground states are full-dimensional structures 4a, 4b, and 5, as well as mixtures of structures 4a and 5. Structure 4b mixes neither with structure 4a nor with structure 5. The disorder in this face is one dimensional.

In face $\{\mathbf{r}_6, \mathbf{r}_7\}$ the ground states are full-dimensional structures $\bar{1}$, 2, 4b, and 5, mixtures of structures $\bar{1}$ and 5 and a two-domain structure. Structures 2 and 4b do not mix with each other and with other structures in this face. The disorder is one dimensional.

In face $\{\mathbf{r}_{12}, \mathbf{r}_{13}\}$ the ground states are full-dimensional structures 6, 10, and 12 which do not intermix.

VI. DIMENSIONALITY OF DISORDER AND RESIDUAL ENTROPY

We already analyzed the dimensionality of disorder and the residual entropy when considering the ground states in the hyperfaces and faces, but this issue is worth being considered in full detail.

The following general statements are obvious. The disorder in an i -face cannot be greater than the disorder in a k -face which bounds this i -face ($i > k$); the disorder in a k -face can not be less than the disorder in an i -face which is bounded by this k -face ($i > k$).

If, in a ground-state structure in an i -face, some local changes can be made in such a manner that the new structure would also be a ground-state one, then, in the i -face, there is a full-dimensional disorder and, hence, a residual entropy per site.

In all basic rays, except \mathbf{r}_1 , the disorder is two dimensional. In ray \mathbf{r}_1 there is no disorder at all; only full-dimensional structures 1, $\bar{1}$, 3, and $\bar{3}$, which do not intermix, are the ground-states there. Certainly, in all faces and hyperfaces bounded by basic ray \mathbf{r}_1 , there is no disorder all the more.

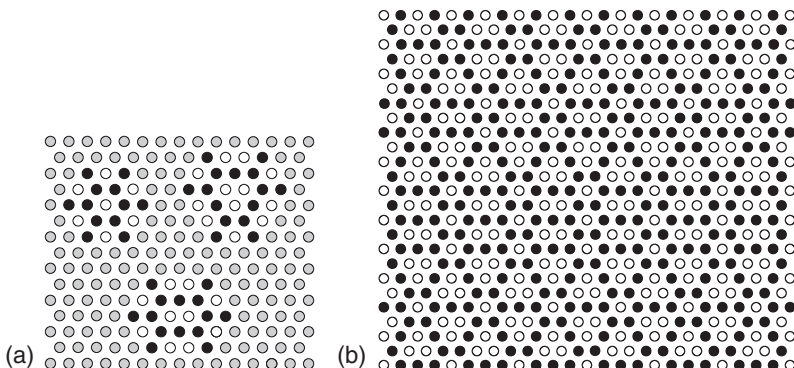


FIG. 16. (a) Blocks which generate the structures in face $\{\mathbf{r}_{10}, \mathbf{r}_{11}\}$ (except for the mixture of phase 3 and 6). (b) A disordered structure in face $\{\mathbf{r}_{10}, \mathbf{r}_{11}\}$.

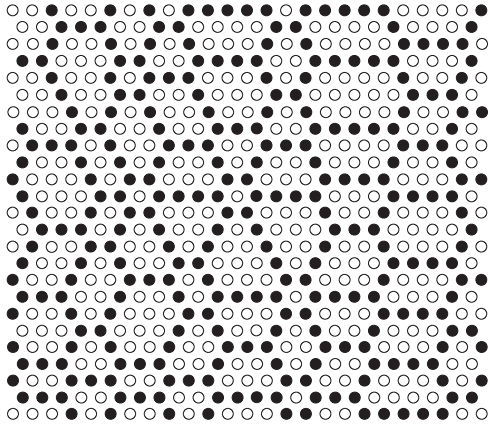


FIG. 17. Hexagonal tiling of the plane in the ground-state structures in face $\{\mathbf{r}_4, \mathbf{r}_{10}\}$.

It is rather easy to prove the existence of two-dimensional disorder in the basic rays. It suffices to find a ground-state structure in which local changes can be made in such a manner that it remains a ground-state structure. It is difficult to find such a structure only for ray \mathbf{r}_{13} . In this ray the disorder is the same as in face $\{\mathbf{r}_4, \mathbf{r}_{13}\}$ since configuration $\odot\odot\odot$ enters only in structure 6, which does not mix with other structures in the ray. A ground-state structure in face $\{\mathbf{r}_4, \mathbf{r}_{13}\}$ is shown in Fig. 18. In this structure every “windmill” can change the orientation independently of other “windmills” and the structure remains a ground-state one. Hence, in this face the disorder is two dimensional.

Residual entropy (two-dimensional disorder) also exists in many hyperfaces (see Table III). These are the hyperfaces (1, 2), (1, 4*b*), (2, 6), (2, 9), (4*a*, 9), and (4*b*, 9). The structure that proves the existence of two-dimensional disorder in the hyperface (4*b*, 9) is shown in Fig. 19. One site from each pair of next-nearest-neighbor gray sites should be filled and another should be open.

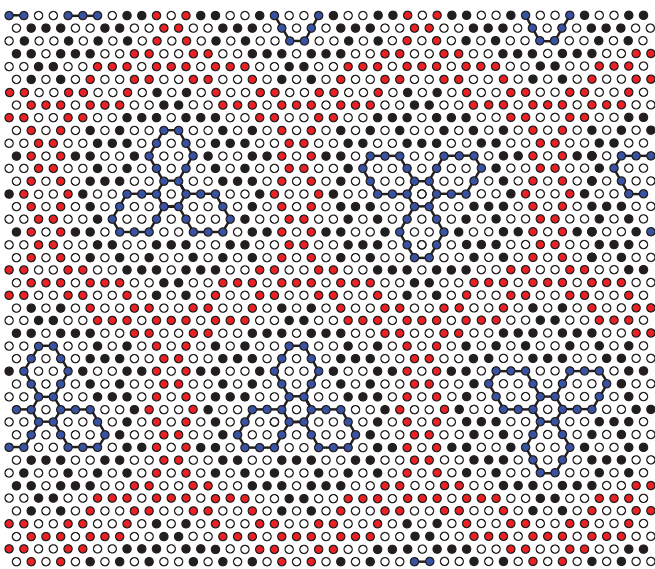


FIG. 18. (Color online) Ground-state structure which proves that there is a residual entropy per site in face $\{\mathbf{r}_4, \mathbf{r}_{13}\}$. The orientation of every “windmill” is arbitrary.

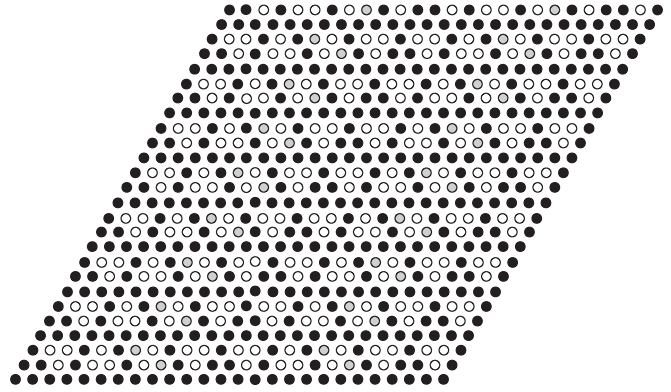


FIG. 19. The proof that in the hyperface (4*b*, 9) a residual entropy exists. One site from each pair of next-nearest-neighbor gray sites should be filled and another open.

Figure 19 makes it possible to calculate a lower bound for the residual entropy in the hyperface (4*b*, 9). As one can see, every 33rd site is completely “free”; that is, it can be occupied or vacant, hence, the residual entropy is greater than $\frac{1}{33} \ln 2 \approx 0.021$. (This value is not exact, since, in the hyperface (4*b*, 9), there are also other structures in addition to those depicted in Fig. 19 and their contribution in the entropy is not zero). In such a simple way one can estimate the residual entropy on every hyperface, face, and ray where the disorder is two dimensional. However, exact calculation of the residual entropy is a very difficult problem and we do not discuss it here.

Ground states in the most part of hyperfaces are generated only with these configurations which generate full-dimensional structures in regions bounded by these hyperfaces. However, for some hyperfaces there are additional configurations which even change the dimensionality of disorder and the order of phase transition. For instance, if it were not configuration $\odot\odot\odot$ in the hyperface (1, 2) or configuration $\odot\odot\odot$ in the hyperface (3, 6), then the transition between corresponding phases would be of the first order. Additional configuration $\odot\odot\odot$ leads to two-dimensional disorder in the hyperface (1, 2) and additional configuration $\odot\odot\odot$ creates one-dimensional disorder in the hyperface (3, 6). A similar situation occurs in the hyperplane (2, 6) where there is two-dimensional disorder: If it were not configuration $\odot\odot\odot$ (configuration $\odot\odot\odot$ cannot be realized in this set without configuration $\odot\odot\odot$), then the transition between these phases would be of the first order.

As one can see from the previous analysis, the existence of a disorder does not ensure the nonzero entropy density; the dimensionality of the disorder should be equal to the dimensionality of the lattice. In view of this fact, the definition of the irregularly ordered ground states given in Ref. [9] (“we define irregularly ordered ground states as those which have no δ peaks in their Fourier transform and whose entropy density is zero”) is not quite correct.

VII. GROUND-STATE PHASE DIAGRAMS

A. Construction of the ground-state phase diagrams in the plane (h, J_2)

Knowing the faces and hyperfaces of the full-dimensional regions, it is easy to construct two-dimensional ground-state

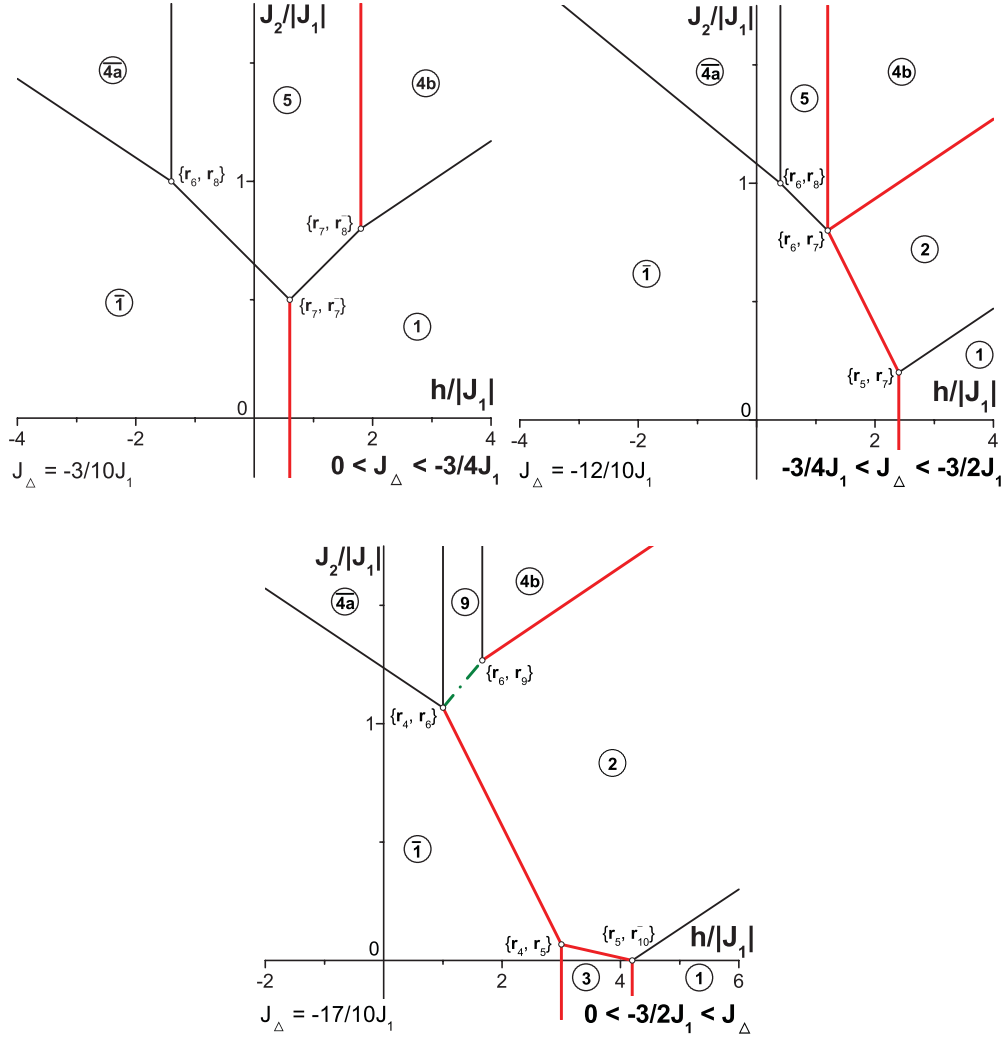


FIG. 20. (Color online) Ground-state phase diagrams in the plane (h, J_2) for the spin model on the triangular lattice with pairwise interactions of nearest and next-nearest neighbors and with three-spin interaction of nearest neighbors. $J_1 < 0$. Red lines correspond to the first-order phase transitions; the green dash-dotted line corresponds to a jump together with a continuous transition.

phase diagrams in any plane, for instance, in the plane (h, J_2) . To do so one should find the intersections of 2-faces with the hyperplanes $J_1 = \text{const}$ and $J_\Delta = \text{const}$.

Let us write, for instance, the equation of the 2-face which is bounded by rays \mathbf{r}_i and \mathbf{r}_j :

$$q_1 \mathbf{r}_i + q_2 \mathbf{r}_j = \mathbf{r}, \quad (26)$$

where q_1 and q_2 are arbitrary non-negative numbers and $\mathbf{r} = (h, J_1, J_2, J_\Delta)^T$ is the column vector of the spin Hamiltonian parameters.

We can first determine q_1 and q_2 and then h and J_2 :

$$q_1 = \frac{r_{j4}J_1 - r_{j2}J_\Delta}{r_{i2}r_{j4} - r_{j2}r_{i4}}, \quad q_2 = -\frac{r_{i4}J_1 - r_{i2}J_\Delta}{r_{i2}r_{j4} - r_{j2}r_{i4}}, \quad (27)$$

$$h = \frac{(r_{i1}r_{j4} - r_{j1}r_{i4})J_1 - (r_{i1}r_{j2} - r_{j1}r_{i2})J_\Delta}{r_{i2}r_{j4} - r_{j2}r_{i4}}, \quad (28)$$

$$J_2 = \frac{(r_{i3}r_{j4} - r_{j3}r_{i4})J_1 - (r_{i2}r_{j3} - r_{j2}r_{i3})J_\Delta}{r_{i2}r_{j4} - r_{j2}r_{i4}}.$$

It is the sought-for point in the plane (h, J_2) . The conditions for its existence are

$$q_1 > 0, \quad q_2 > 0. \quad (29)$$

Let us consider a face for which the denominator $r_{i2}r_{j4} - r_{j2}r_{i4}$ is equal to zero (first ten faces in Table II), for instance, face $\{\mathbf{r}_1, \mathbf{r}_5\}$. The set of equations (26) reads, in this case,

$$6q_2 = h, \quad -2q_2 = J_1, \quad -q_1 = J_2, \quad 3q_2 = J_\Delta, \quad (30)$$

whence we have

$$q_1 = -J_2, \quad q_2 = \frac{1}{6}h = -\frac{1}{2}J_1 = \frac{1}{3}J_\Delta. \quad (31)$$

We obtained ray $h = -3J_1, J_2 < 0$ lying in the plane (h, J_2) if $J_\Delta = -\frac{3}{2}J_1$ ($J_1 < 0$) or parallel to this plane otherwise. One can say that this ray intersects the plane (h, J_2) in the point that is infinitely distant in the negative direction of axis J_2 . The same holds true for symmetric face $\{\mathbf{r}_1, \mathbf{r}_5^-\}$ as well as for the pair of faces $\{\mathbf{r}_1, \mathbf{r}_{10}^-\}$ and $\{\mathbf{r}_1, \mathbf{r}_{10}\}$. All these four infinitely distant points can be considered either separately

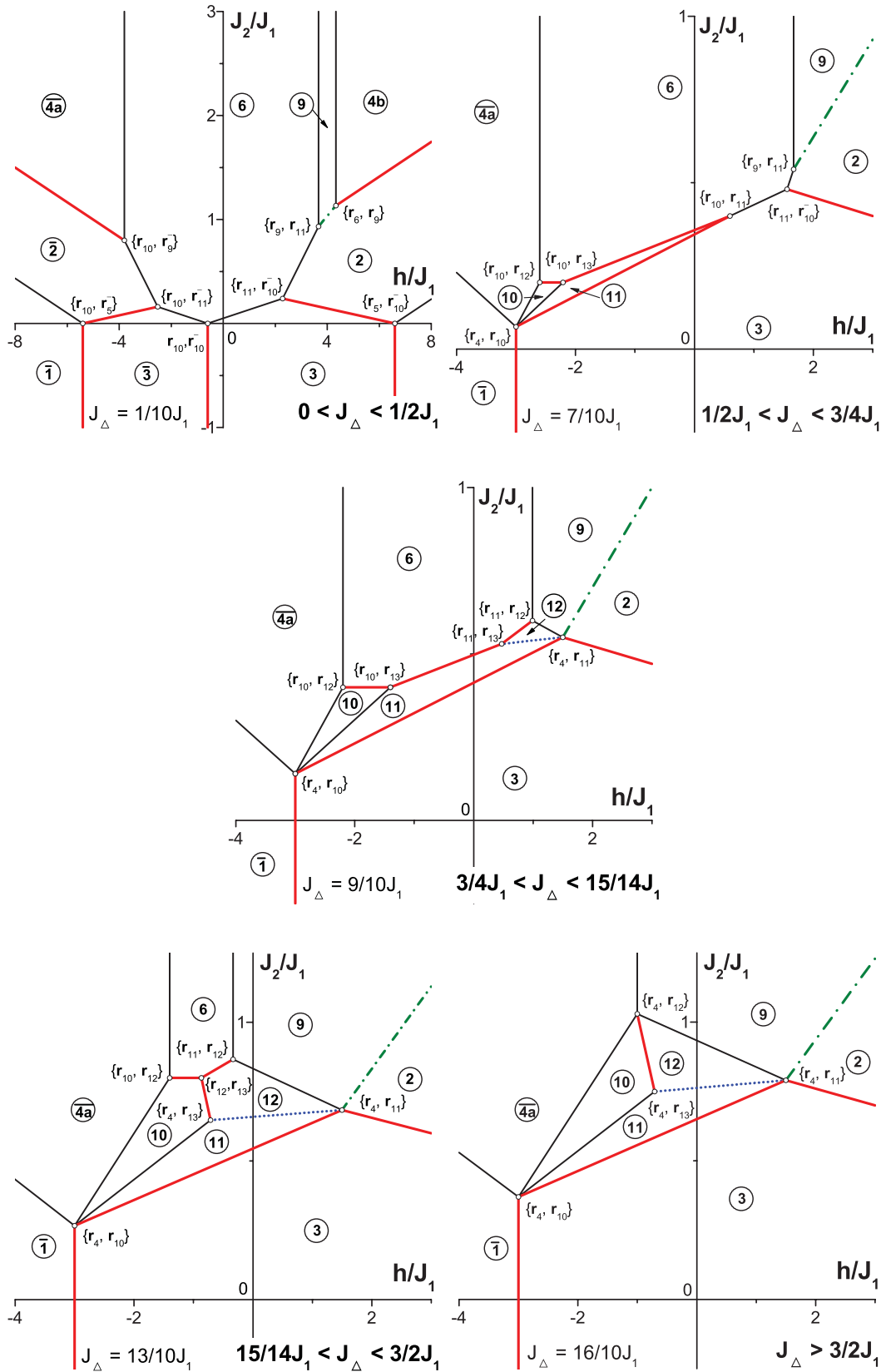


FIG. 21. (Color online) Ground-state phase diagrams in the plane (h, J_2) for the spin model on the triangular lattice with pairwise interactions of nearest and next-nearest neighbors and with three-spin interaction of nearest neighbors. $J_1 > 0$. Red lines correspond to the first-order phase transitions, the green dash-dotted line corresponds to a jump together with a continuous transition, and the blue dotted line corresponds to a cascade of first-order phase transitions.

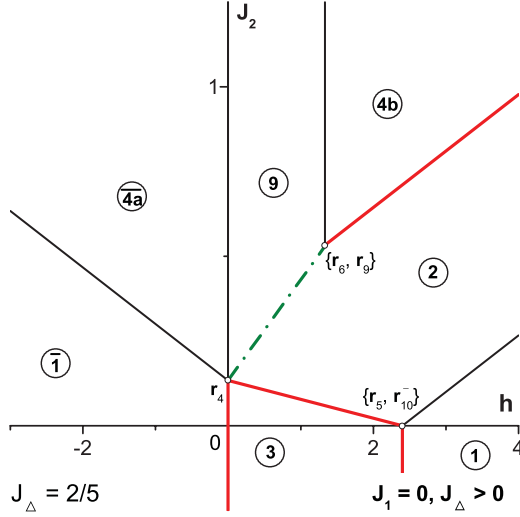


FIG. 22. (Color online) Ground-state phase diagrams in the plane (h, J_2) for the spin model on the triangular lattice with pairwise interactions of nearest and next-nearest neighbors and with three-spin interaction of nearest neighbors. $J_1 = 0$. Red lines correspond to the first-order phase transitions; the green dash-dotted line corresponds to a jump together with a continuous transition.

with their sets of flower configurations or as a unique point with the set which is the union of all four sets of flower configurations.

Considering all ten initial faces in Table II and ten symmetric faces, we obtain four “infinite” points in the plane (h, J_2) : in negative direction of axis J_2 , in positive direction of this axis, in direction $\frac{h}{J_2} = 6$ ($h > 0$), and in direction $\frac{h}{J_2} = -6$ ($h < 0$). These points correspond to the basic vectors \mathbf{r}_1 , \mathbf{r}_2 , \mathbf{r}_3 , and \mathbf{r}_3^- , which are parallel to the plane (h, J_2) ($J_1 = \text{const}$, $J_\Delta = \text{const}$).

Now we can show the way of determining the intersection of a hyperface by the hyperplanes $J_1 = \text{const}$ and $J_\Delta = \text{const}$ and the conditions for its existence. We should obtain a ray or a segment. Let us consider, for instance, the hyperplane bounded by the triplet of rays \mathbf{r}_4 , \mathbf{r}_{10} , and \mathbf{r}_{11} . This hyperface is the boundary between regions 3 and 11. The equation of the hyperface reads

$$q_1 \mathbf{r}_4 + q_2 \mathbf{r}_{10} + q_3 \mathbf{r}_{11} = \mathbf{r}, \quad (32)$$

where q_1 , q_2 , and q_3 are arbitrary non-negative numbers. From this set of equations we obtain

$$\begin{aligned} 5h &= -6J_1 + 54J_2 - 18J_\Delta, \\ 5q_1 &= -J_1 - J_2 + 2J_\Delta, \\ 10q_2 &= 3J_1 - 12J_2 + 4J_\Delta, \\ 10q_3 &= J_1 + 6J_2 - 2J_\Delta. \end{aligned} \quad (33)$$

Conditions of non-negativity of coefficients q_1 , q_2 , and q_3 leads to the following set of inequalities:

$$\begin{aligned} J_1 + J_2 - 2J_\Delta &< 0, \\ -3J_1 + 12J_2 - 4J_\Delta &< 0, \\ -J_1 - 6J_2 + 2J_\Delta &< 0. \end{aligned} \quad (34)$$

This set together with equation $5h + 6J_1 - 54J_2 + 18J_\Delta = 0$ define the hyperface. The set of inequalities has solutions if the following conditions hold true:

$$-J_1 < 0, \quad J_1 - 2J_\Delta < 0. \quad (35)$$

These are conditions for the existence of a boundary between regions 3 and 11 in the plane (h, J_2) . The similar conditions are presented in Table III.

Now we can construct ground-state phase diagrams in the plane (h, J_2) for the spin model on the triangular lattice with pairwise interactions of nearest and next-nearest neighbors and with three-spin interaction of nearest and nearest neighbors. They are shown in Figs. 20–22. There are nine different diagrams. They are not symmetric with respect to the inversion of the external field h (as it is in the $J_\Delta = 0$ case [4]). The boundaries between phases where there are first-order phase transitions are marked in red.

B. How to find ground-state structure at fixed interactions and density of particles

We considered ground states of spin Hamiltonian (2) with the external field or of equivalent lattice-gas Hamiltonian (1) with the chemical potential. Now we are able to determine the ground states of model (1) in the case of fixed density of particles.

Let the density of particles p_0 (the number of particles per site) and the interaction parameters I_1 , I_2 , and I_Δ be fixed. What are the ground states of such a system? The following statement provides the answer to this question: If for fixed p_0 , I_1 , I_2 , and I_Δ there exists such a value of the chemical potential μ_{lg} of model (1) that corresponding ground-state structures without defects have the density of particles equal to p_0 , then these structures are the sought-for ground-state structures. If model (1) does not possess such ground-state structures without defects, then the ground state of the system is phase separated. It contains domains of the structures which have the densities of particles closest to p_0 in such a proportion that the average density is equal to p_0 . A phase-separated ground state contains flower configurations (included in domain walls) with nonminimal energy but their quantity is infinitesimal with respect to the quantity of flower configurations with the minimal energy. It is natural to suppose that the domain walls should be of the form which minimizes the linear density of energy. However, this complicated problem is not a subject of the present work.

Usually the dimensionality of disorder at a fixed density of particles is the same as at fixed chemical potential but not always. We did not try to find a case where this is not so in the model under consideration.

VIII. CONCLUSIONS

We considered the ground-state problem of the lattice-gas model (or the equivalent spin one) on the triangular lattice with pairwise interactions of nearest and next-nearest neighbors and with three-particle interaction of nearest neighbors. Using the solution of this problem found in the previous paper [3], we constructed and analyzed ground-state structures at all three-dimensional boundaries of the full-dimensional regions in the Hamiltonian parameter space, except for two mutually

symmetric boundaries where the ground states were analyzed only partially. It enabled us to analyze the phase transitions between the full-dimensional phases. We also found the dimensionality of disorder for all boundaries. To facilitate the use of our results we constructed the ground-state phase diagrams in the (h, J_2) plane. Hence, this ground-state problem can be considered as completely solved and the researchers dealing with this model can use our results. True, it remains to

find ground states at the boundary between phases 9 and 12. However, this problem is so complicated and so interesting that it is worthy of a separate study.

ACKNOWLEDGMENTS

The author is grateful to I. Stasyuk, T. Verkholyak, and O. Velychko for helpful discussions and recommendations.

-
- [1] G. H. Wannier, *Phys. Rev.* **79**, 357 (1950); A. Danielian, *Phys. Rev. Lett.* **6**, 670 (1961); J. Kanamori, *Prog. Theor. Phys.* **35**, 16 (1966); T. Kennedy, *Rev. Math. Phys.* **6**, 901 (1994).
- [2] U. Brandt and J. Stolze, *Z. Phys. B* **64**, 481 (1986).
- [3] Yu. I. Dublenych, *Phys. Rev. E* **84**, 011106 (2011).
- [4] Yu. I. Dublenych, *Phys. Rev. E* **80**, 011123 (2009).
- [5] J. Kanamori, *J. Phys. Soc. Jpn.* **53**, 250 (1984).
- [6] M. E. Fisher and W. Selke, *Philos. Trans. R. Soc. London A* **302**, 1 (1981); *Phys. Rev. Lett.* **44**, 1502 (1980).
- [7] M. Kaburagi and J. Kanamori, *J. Phys. Soc. Jpn.* **44**, 718 (1978).
- [8] Yu. I. Dublenych, *Phys. Rev. E* **83**, 022101 (2011).
- [9] Shin-ichi Sasa, *J. Phys. A: Math. Theor.* **43**, 465002 (2010).